Chapter 6 Generalized Conforming Thin Plate Element Ⅱ—Line-Point and SemiLoof Conforming Schemes

Zhi-Fei Long
School of Mechanics & Civil Engineering, China University of Mining & Technology, Beijing, 100083, China

Song Cen
Department of Engineering Mechanics, School of Aerospace, Tsinghua University, Beijing, 100084, China

Abstract Five groups of construction schemes for the generalized conforming thin plate elements are proposed in Sect. 5.4. This chapter discusses the first three groups: (1) line conforming scheme (Sect. 6.1); (2) line-point conforming scheme (Sects. 6.2 and 6.3) and super-basis line-point conforming scheme (Sect. 6.4); and (3) super-basis point conforming scheme (Sect. 6.5) and SemiLoof conforming scheme (Sect. 6.6). Formulations of 13 triangular, rectangular and quadrilateral generalized conforming thin plate elements, which are constructed by the above schemes, are introduced in detail. The elements formulated in Sects. 6.1 to 6.3 belong to the equal-basis elements, in which the number m of the unknown coefficients or basis functions in an interpolation formula for the element deflection field equals to the number n of DOFs. And, the elements formulated in Sects. 6.4 to 6.6 belong to the super-basis elements, in which $m > n$. Numerical examples show that these models exhibit excellent performance in the analysis of thin plates. This denotes that the difficulty of C_1 continuity problem can be solved completely.

Keywords thin plate element, generalized conforming, line-point conforming, SemiLoof conforming.

6.1 Line Conforming Scheme—Elements TGC-9 and TGC-9-1

In this section, the generalized conforming thin plate elements TGC-9 and TGC-9-1 will be taken as examples for illustrating the procedure of the line conforming

scheme. The outlines of the procedure are as follows: all conforming conditions are line conforming ones, especially, the average line conforming conditions (5-22) are taken as the main conditions; for the element TGC-9, let $m=n$; and for the element TGC-9-1, it is extended from the element TGC-9 by introducing an internal parameter α, which will be eliminated by condensation.

6.1.1 Element TGC-9

A triangular thin plate element with 9 DOFs is shown in Fig. 6.1. Its nodal displacement vector $\boldsymbol{q}^e$ is

$$\boldsymbol{q}^e=[w_1 \quad \psi_{x1} \quad \psi_{y1} \quad w_2 \quad \psi_{x2} \quad \psi_{y2} \quad w_3 \quad \psi_{x3} \quad \psi_{y3}]^{\mathrm{T}} \tag{6-1}$$

Along each element side, the deflection $\tilde{w}$ is assumed to be cubic and the normal slope $\tilde{\psi}_n$ linear.

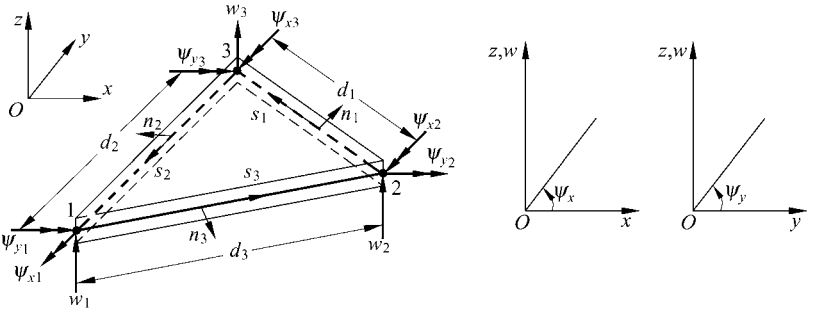

Figure 6.1 A triangular thin plate bending element

According to the element BCIZ in reference [1], the element deflection field $w(x, y)$ is described by an incomplete cubic polynomial and expressed in terms of the area coordinates L_1, L_2, L_3:

$$w=\boldsymbol{F}_\lambda\boldsymbol{\lambda} \tag{6-2}$$

where $\boldsymbol{\lambda}$ is a vector containing 9 unknown coefficients:

$$\boldsymbol{\lambda}=[\lambda_1 \quad \lambda_2 \quad \lambda_3 \quad \lambda_4 \quad \lambda_5 \quad \lambda_6 \quad \lambda_7 \quad \lambda_8 \quad \lambda_9]^{\mathrm{T}}$$

and $\boldsymbol{F}_\lambda$ is a row matrix containing 9 basis functions:

$$\left.\begin{aligned}
&\boldsymbol{F}_\lambda=[L_1 \quad L_2 \quad L_3 \quad F_4 \quad F_5 \quad F_6 \quad F_7 \quad F_8 \quad F_9]\\
&F_4=L_1L_2(L_1+\frac{1}{2}L_3),\quad F_5=L_2L_3(L_2+\frac{1}{2}L_1),\quad F_6=L_3L_1(L_3+\frac{1}{2}L_2)\\
&F_7=L_1L_3(L_1+\frac{1}{2}L_2),\quad F_8=L_2L_1(L_2+\frac{1}{2}L_3),\quad F_9=L_3L_2(L_3+\frac{1}{2}L_1)
\end{aligned}\right\} \tag{6-3}$$

In order to determine the 9 unknown coefficients of $\boldsymbol{\lambda}$ in terms of $\boldsymbol{q}^e$, 9 generalized conforming conditions are needed. Here, the line conforming scheme, especially the average line conforming conditions (5-22), are firstly considered. Each element has three sides, along which the average deflection, average normal slope and average tangential slope conforming conditions are used. So, to outward seeming, there are just 9 generalized conforming conditions here. But, if $w-\tilde{w}$ is a continuous function along the boundary perimeter ∂A^e, the following identity relation

$$\oint_{\partial A^e} \frac{\partial}{\partial s}(w-\tilde{w})\mathrm{d}s = 0 \tag{6-4}$$

will come into existence, i.e.,

$$\sum_{i=1}^{3} \int_{\Gamma_i} \left(\frac{\partial w}{\partial s} - \tilde{\psi}_s \right) \mathrm{d}s = 0 \tag{6-5}$$

Therefore, there are only two independent conditions actually active for the tangential slop ψ_s. That is to say, when Eq. (5-22) is used along each element side, there are only 8 independent generalized conforming conditions, which are the first eight equations of the following equation set:

$$\left.\begin{aligned}
&\int_0^1 w_{23}\mathrm{d}L_3 \equiv d_4 = \int_0^1 \tilde{w}_{23}\mathrm{d}L_3 \\
&\int_0^1 w_{31}\mathrm{d}L_1 \equiv d_5 = \int_0^1 \tilde{w}_{31}\mathrm{d}L_1 \\
&\int_0^1 w_{12}\mathrm{d}L_2 \equiv d_6 = \int_0^1 \tilde{w}_{12}\mathrm{d}L_2 \\
&\int_0^1 \left(\frac{\partial w}{\partial n}\right)_{23} \mathrm{d}L_3 \equiv d_7 = \int_0^1 (\tilde{\psi}_n)_{23}\mathrm{d}L_3 \\
&\int_0^1 \left(\frac{\partial w}{\partial n}\right)_{31} \mathrm{d}L_1 \equiv d_8 = \int_0^1 (\tilde{\psi}_n)_{31}\mathrm{d}L_1 \\
&\int_0^1 \left(\frac{\partial w}{\partial n}\right)_{12} \mathrm{d}L_2 \equiv d_9 = \int_0^1 (\tilde{\psi}_n)_{12}\mathrm{d}L_2 \\
&\int_0^1 \left(\frac{\partial w}{\partial s}\right)_{23} \mathrm{d}L_3 \equiv d_1 = \int_0^1 (\tilde{\psi}_s)_{23}\mathrm{d}L_3 \\
&\int_0^1 \left(\frac{\partial w}{\partial s}\right)_{31} \mathrm{d}L_1 \equiv d_2 = \int_0^1 (\tilde{\psi}_s)_{31}\mathrm{d}L_1 \\
&\int_0^1 w_{23}\left(L_3-\frac{1}{2}\right)\mathrm{d}L_3 + \int_0^1 w_{31}\left(L_1-\frac{1}{2}\right)\mathrm{d}L_1 + \int_0^1 w_{12}\left(L_2-\frac{1}{2}\right)\mathrm{d}L_2 \equiv d_3 \\
&= \int_0^1 \tilde{w}_{23}\left(L_3-\frac{1}{2}\right)\mathrm{d}L_3 + \int_0^1 \tilde{w}_{31}\left(L_1-\frac{1}{2}\right)\mathrm{d}L_1 + \int_0^1 \tilde{w}_{12}\left(L_2-\frac{1}{2}\right)\mathrm{d}L_2
\end{aligned}\right\} \tag{6-6}$$

The ninth equation in Eq. (6-6) is the supplementary generalized conforming condition, which denotes the generalized conforming condition that the sum of the first moments of the deflections along three sides should satisfy.

By using the symbol of Eq. (5-13) and arranging in the sequence of d_1, d_2, $\cdots$, d_9, Eq. (6-6) can be rewritten in the following matrix form:

$$\hat{\boldsymbol{C}}\boldsymbol{\lambda} = \hat{\boldsymbol{G}}\boldsymbol{q}^{e} \tag{6-7}$$

where

$$\hat{\boldsymbol{G}} = \begin{bmatrix} 0 & 0 & 0 & -1 & 0 & 0 & 1 & 0 & 0 \\ 1 & 0 & 0 & 0 & 0 & 0 & -1 & 0 & 0 \\ 0 & c_1 & -b_1 & 0 & c_2 & -b_2 & 0 & c_3 & -b_3 \\ 0 & 0 & 0 & 6 & c_1 & -b_1 & 6 & -c_1 & b_1 \\ 6 & -c_2 & b_2 & 0 & 0 & 0 & 6 & c_2 & -b_2 \\ 6 & c_3 & -b_3 & 6 & -c_3 & b_3 & 0 & 0 & 0 \\ 0 & 0 & 0 & 0 & b_1 & c_1 & 0 & b_1 & c_1 \\ 0 & b_2 & c_2 & 0 & 0 & 0 & 0 & b_2 & c_2 \\ 0 & b_3 & c_3 & 0 & b_3 & c_3 & 0 & 0 & 0 \end{bmatrix} \tag{6-8}$$

$$\hat{\boldsymbol{C}} = \begin{bmatrix} 0 & -1 & 1 & 0 & 0 & 0 & 0 & 0 & 0 \\ 1 & 0 & -1 & 0 & 0 & 0 & 0 & 0 & 0 \\ 0 & 0 & 0 & -1 & -1 & -1 & 1 & 1 & 1 \\ 0 & 6 & 6 & 0 & 1 & 0 & 0 & 0 & 1 \\ 6 & 0 & 6 & 0 & 0 & 1 & 1 & 0 & 0 \\ 6 & 6 & 0 & 1 & 0 & 0 & 0 & 1 & 0 \\ & \hat{\boldsymbol{C}}_1 & & & \hat{\boldsymbol{C}}_2 & & & \hat{\boldsymbol{C}}_3 & \end{bmatrix} \tag{6-9}$$

and

$$\hat{\boldsymbol{C}}_1 = \begin{bmatrix} \dfrac{f_2+f_3}{A} & -\dfrac{f_3}{A} & -\dfrac{f_2}{A} \\ -\dfrac{f_3}{A} & \dfrac{f_3+f_1}{A} & -\dfrac{f_1}{A} \\ -\dfrac{f_2}{A} & -\dfrac{f_1}{A} & \dfrac{f_1+f_2}{A} \end{bmatrix} \tag{6-10}$$

$$\hat{\boldsymbol{C}}_2 = \begin{bmatrix} \frac{f_2+f_3}{12A} & -3\frac{f_2+f_3}{12A} & 5\frac{f_2+f_3}{12A} \\ 5\frac{f_3+f_1}{12A} & \frac{f_3+f_1}{12A} & -3\frac{f_3+f_1}{12A} \\ -3\frac{f_1+f_2}{12A} & 5\frac{f_1+f_2}{12A} & \frac{f_1+f_2}{12A} \end{bmatrix} \tag{6-11}$$

$$\hat{\boldsymbol{C}}_3 = \begin{bmatrix} \frac{f_2+f_3}{12A} & 5\frac{f_2+f_3}{12A} & -3\frac{f_2+f_3}{12A} \\ -3\frac{f_3+f_1}{12A} & \frac{f_3+f_1}{12A} & 5\frac{f_3+f_1}{12A} \\ 5\frac{f_1+f_2}{12A} & -3\frac{f_1+f_2}{12A} & \frac{f_1+f_2}{12A} \end{bmatrix} \tag{6-12}$$

in which A is the area of the triangle; and

$$\left.\begin{aligned} b_i &= y_j - y_k \\ c_i &= x_k - x_j \\ f_i &= -(b_j b_k + c_j c_k) \end{aligned}\right\} \quad (i = \overrightarrow{1,2,3};\quad j = \overrightarrow{2,3,1};\quad k = \overrightarrow{3,1,2}) \tag{6-13}$$

It can be verified that $\hat{\boldsymbol{G}}$ and $\hat{\boldsymbol{C}}$ are not singular. So, from Eqs. (6-7) and (6-2), we have

$$w = \boldsymbol{F}_\lambda \hat{\boldsymbol{C}}^{-1} \hat{\boldsymbol{G}} \boldsymbol{q}^e$$

Then, the element stiffness matrix can be obtained following the standard procedure.

6.1.2 Element TGC-9-1

Assume that the element deflection field w is constituted of two parts

$$w = w_q + w_\alpha \tag{6-14}$$

where the first part is the deflection field expressed in Eq. (6-2)

$$w_q = \boldsymbol{F}_\lambda \boldsymbol{\lambda} = \boldsymbol{F}_\lambda (\hat{\boldsymbol{C}}^{-1} \hat{\boldsymbol{G}}) \boldsymbol{q}^e \tag{6-15}$$

The second part is a generalized bubble deflection field

$$w_\alpha = F_\alpha \alpha \tag{6-16}$$

where α is an internal displacement parameter and F_α is a generalized bubble function:

$$F_\alpha = 1 - 6(L_1L_2 + L_2L_3 + L_3L_1) + 18L_1L_2L_3 \tag{6-17}$$

It can be verified that all the 9 generalized displacements $d_1, \cdots, d_9$ corresponding to w_α vanish.

The deflection field (6-14) is a complete cubic polynomial with 10 DOFs. α is eliminated by a condensation process, only 9 external DOFs in $\boldsymbol{q}^e$ are retained.

From the expression (6-14) of the deflection field, the curvature field $\boldsymbol{\kappa}$ can be expressed as

$$\boldsymbol{\kappa} = \left[-\frac{\partial^2 w}{\partial x^2} \quad -\frac{\partial^2 w}{\partial y^2} \quad -2\frac{\partial^2 w}{\partial x \partial y} \right]^{\mathrm{T}} = \boldsymbol{B}\boldsymbol{q}^e + \boldsymbol{B}_\alpha \alpha \tag{6-18}$$

and the element strain energy U is

$$U = \frac{1}{2}\iint_{A^e} \boldsymbol{\kappa}^{\mathrm{T}} \boldsymbol{D}\boldsymbol{\kappa} \mathrm{d}A = \frac{1}{2}\boldsymbol{q}^{e\mathrm{T}} \boldsymbol{K}_{qq}{}^e \boldsymbol{q}^e + \alpha \boldsymbol{K}_{\alpha q}\boldsymbol{q}^e + \frac{1}{2}\alpha^2 k_{\alpha\alpha} \tag{6-19}$$

where

$$\left.\begin{aligned} \boldsymbol{K}_{qq} &= \iint_{A^e} \boldsymbol{B}^{\mathrm{T}} \boldsymbol{D}\boldsymbol{B} \mathrm{d}A \\ \boldsymbol{K}_{\alpha q} &= \iint_{A^e} \boldsymbol{B}_\alpha{}^{\mathrm{T}} \boldsymbol{D}\boldsymbol{B} \mathrm{d}A \\ k_{\alpha\alpha} &= \iint_{A^e} \boldsymbol{B}_\alpha{}^{\mathrm{T}} \boldsymbol{D}\boldsymbol{B}_\alpha \mathrm{d}A \end{aligned}\right\} \tag{6-20}$$

Applying a condensation process, we can solve α from $\dfrac{\partial U}{\partial \alpha} = 0$:

$$\alpha = -k_{\alpha\alpha}^{-1} \boldsymbol{K}_{\alpha q}\boldsymbol{q}^e$$

Substitution of the above equation into Eq. (6-19) yields

$$U = \frac{1}{2}\boldsymbol{q}^{e\mathrm{T}} \boldsymbol{K}^e \boldsymbol{q}^e$$

where $\boldsymbol{K}^e$ is the element stiffness matrix after condensation:

$$\boldsymbol{K}^e = \boldsymbol{K}_{qq} - \boldsymbol{K}_{\alpha q}{}^{\mathrm{T}} k_{\alpha\alpha}^{-1} \boldsymbol{K}_{\alpha q} \tag{6-21}$$

6.1.3 Numerical Examples

Example 6.1 Simply-supported and clamped square plates subjected to uniformly distributed load q or central concentrated load P—comparison of five triangular thin plate elements. L is the length of the plate side; and Poisson's ratio $\mu = 0.3$.

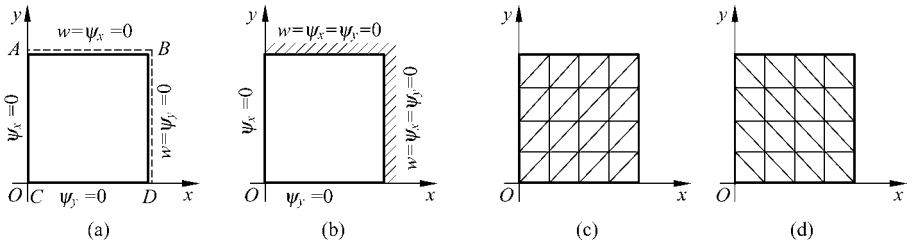

Figure 6.2 Meshes for a quarter square plate

(a) A quarter simply-supported square plate; (b) A quarter clamped square plate; (c) Mesh orientation *A* Mesh density $N = 4$; (d) Mesh orientation *B* Mesh density $N = 4$

Owing to symmetry, only one-quarter of the plate is modelled. As shown in Fig. 6.2, two mesh orientations (*A* and *B*) are considered. For comparison, the results by the five triangular element models with 9 DOFs, the generalized conforming element TGC-9-1, the discrete Kirchhoff theory element DKT[2, 3], the hybrid-stress element HSM[2,4], the non-conforming element BCIZ[1] and the conforming element HCT[5], are given together.

The results of the central deflection w_C for the uniformly distributed load case are plotted in Figs. 6.3 and 6.4. And, the results for the concentrated load case are given in Figs. 6.5 and 6.6. Among the five elements used, the generalized conforming element TGC-9-1 gives the most accurate answers, and the elements HSM and DKT give the second best ones.

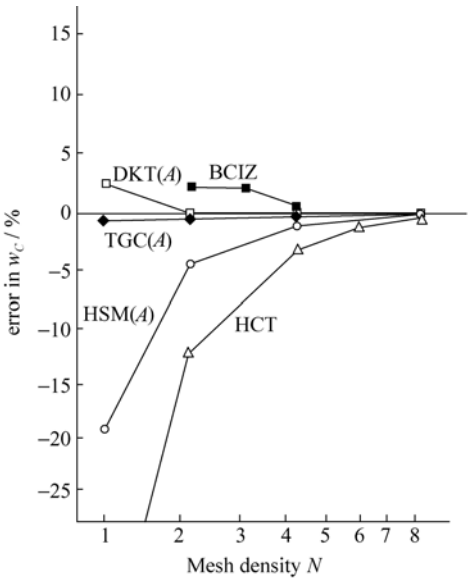

Figure 6.3 The percentage error for central deflection of the simply-supported square plate subjected to uniform load

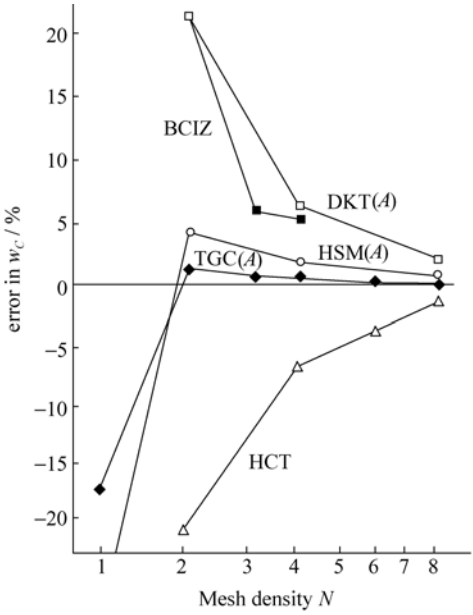

Figure 6.4 The percentage error for central deflection of the clamped square plate subjected to uniform load

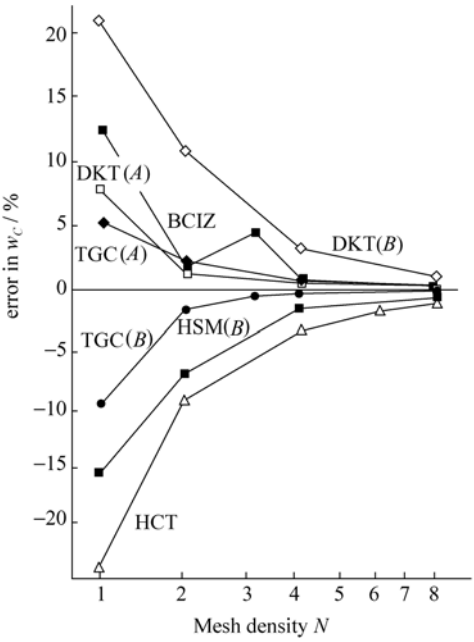

Figure 6.5 The percentage error for central deflection of the simply-supported square plate subjected to concentrated load

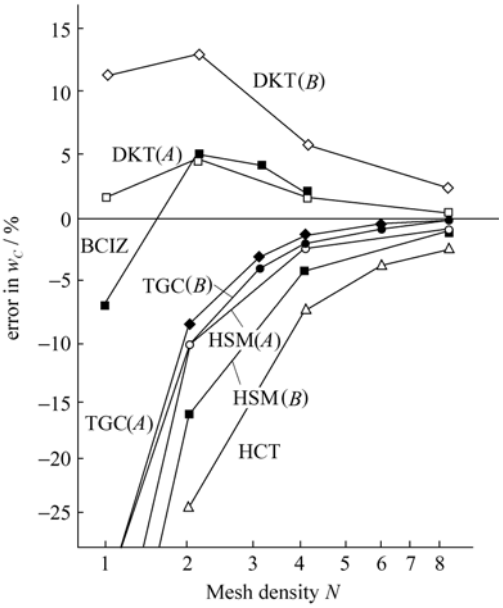

Figure 6.6 The percentage error for central deflection of the clamped square plate subjected to concentrated load

The results of the central moment M_C are given in Figs. 6.7 and 6.8. The accuracy of the generalized conforming element is still the best. And, the results

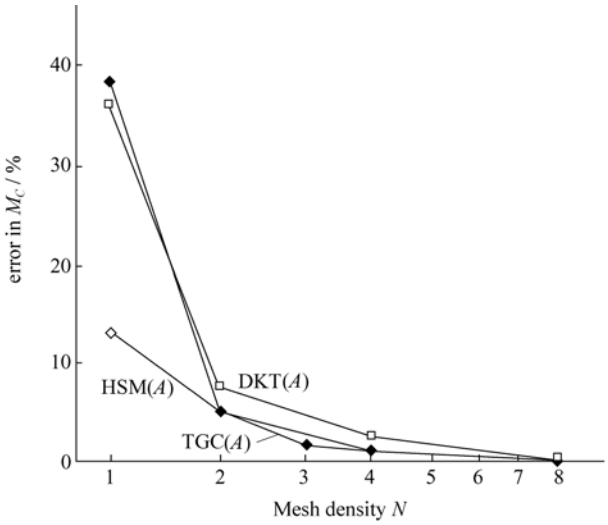

Figure 6.7 The percentage error for central moment of the simply-supported square plate subjected to uniform load

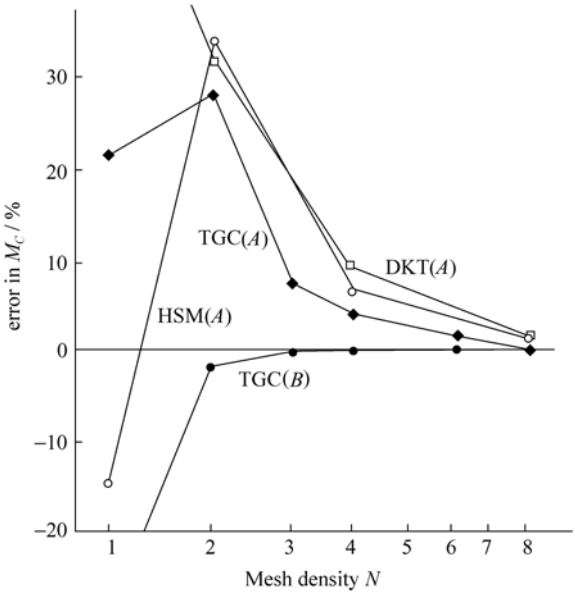

Figure 6.8 The percentage error for central moment of the clamped square plate subjected to uniform load

of the moment M_D at the mid-side point of the plate are given in Figs. 6.9 and 6.10. The elements TGC, HSM and DKT are at the same level of accuracy.

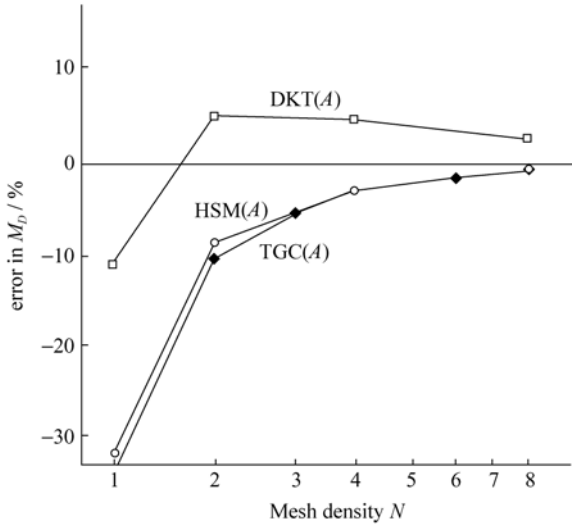

Figure 6.9 The percentage error for moment at mid-side point of the clamped square plate subjected to uniform load

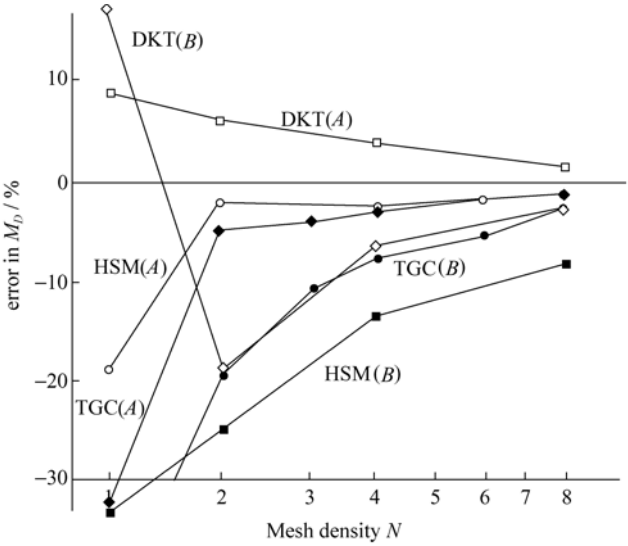

Figure 6.10 The percentage error for moment at mid-side point of the clamped square plate subjected to concentrated load

Different mesh orientations lead to different results for these elements, and the smallest difference is obtained by the generalized conforming element.

6.2 Line-Point Conforming Scheme—Rectangular Elements

The mixed scheme of line and point conforming is one of the most popular schemes for constructing the generalized conforming thin plate elements. We will introduce it in two sections: rectangular elements in this section and triangular elements in the next.

The no. 3, 4, 5 elements RGC-12, CGC-R12 and LGC-R12 in Table 5.1 are all rectangular elements constructed by the line-point conforming scheme, in which $m = n = 12$. Besides, some other contents, including the simplification by using the symmetry of rectangular elements, and the buckling analysis of thin plates, are also introduced.

6.2.1 Rectangular Element RGC-12 (Bending Problem)

A 12-DOF rectangular thin plate element is shown in Fig. 6.11. The element nodal displacement vector $\boldsymbol{q}^e$ is

$$\boldsymbol{q}^e = [w_1 \quad \psi_{x1} \quad \psi_{y1} \quad w_2 \quad \psi_{x2} \quad \psi_{y2} \quad w_3 \quad \psi_{x3} \quad \psi_{y3} \quad w_4 \quad \psi_{x4} \quad \psi_{y4}]^{\mathrm{T}}$$

where w denotes the deflection; $\psi_x = \dfrac{\partial w}{\partial x}$ and $\psi_y = \dfrac{\partial w}{\partial y}$ denote the rotations.

Along each element side, the deflection $\tilde{w}$ is assumed to be cubic and the normal slope $\tilde{\psi}_n$ linearly distributed.

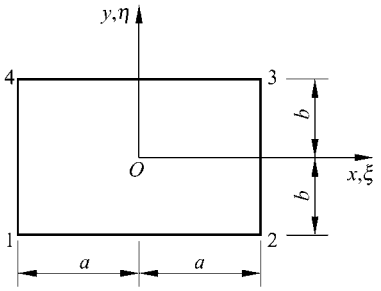

Figure 6.11 Rectangular plate

Let ξ, η be the dimensionless coordinates: $\xi = \dfrac{x}{a}$, $\eta = \dfrac{y}{b}$.

According to the element ACM[6], the element deflection field w is described by an incomplete quartic polynomial

$$w = \boldsymbol{F}_\lambda \boldsymbol{\lambda} \tag{6-22}$$

in which

$$\left.\begin{aligned} \boldsymbol{\lambda} &= [\lambda_1 \quad \lambda_2 \quad \lambda_3 \quad \lambda_4 \quad \lambda_5 \quad \lambda_6 \quad \lambda_7 \quad \lambda_8 \quad \lambda_9 \quad \lambda_{10} \quad \lambda_{11} \quad \lambda_{12}]^{\mathrm{T}} \\ \boldsymbol{F}_\lambda &= [1 \quad \xi \quad \eta \quad \xi^2 \quad \xi\eta \quad \eta^2 \quad \xi^3 \quad \xi^2\eta \quad \xi\eta^2 \quad \eta^3 \quad \xi^3\eta \quad \xi\eta^3] \end{aligned}\right\} \tag{6-23}$$

In order to solve $\boldsymbol{\lambda}$, it is necessary to choose 12 generalized conforming conditions and their corresponding generalized displacements $\boldsymbol{d}$.

$$\boldsymbol{d} = [d_1 \quad d_2 \quad d_3 \quad d_4 \quad d_5 \quad d_6 \quad d_7 \quad d_8 \quad d_9 \quad d_{10} \quad d_{11} \quad d_{12}]^{\mathrm{T}}$$

First of all, we consider the average deflection, the average tangential slope and the average normal slope of each element side, thus 12 average displacements are involved. But, there are two identity relations for these quantities, so only 10 of the average displacements are independent, which may be chosen as the first ten generalized displacements d_1, $d_2, \cdots$, d_{10}. And, the rotations of node 1, ψ_{x1}

and ψ_{y1}, could be chosen as the other two generalized displacements d_{11} and d_{12}. Thus, 12 generalized conforming conditions are established as follows:

$$\left.\begin{aligned}
&\int_{-1}^{1}\left(\frac{\partial w}{\partial y}\right)_{12}\mathrm{d}\xi = d_1 = \int_{-1}^{1}\overline{\psi}_{y12}\mathrm{d}\xi\\
&\int_{-1}^{1}\left(\frac{\partial w}{\partial x}\right)_{23}\mathrm{d}\eta = d_2 = \int_{-1}^{1}\overline{\psi}_{x23}\mathrm{d}\eta\\
&\int_{-1}^{1}\left(\frac{\partial w}{\partial y}\right)_{43}\mathrm{d}\xi = d_3 = \int_{-1}^{1}\overline{\psi}_{y43}\mathrm{d}\xi\\
&\int_{-1}^{1}\left(\frac{\partial w}{\partial x}\right)_{14}\mathrm{d}\eta = d_4 = \int_{-1}^{1}\overline{\psi}_{x14}\mathrm{d}\eta\\
&\int_{-1}^{1}\left(\frac{\partial w}{\partial x}\right)_{12}\mathrm{d}\xi = d_5 = \int_{-1}^{1}\left(\frac{\partial \tilde{w}}{\partial x}\right)_{12}\mathrm{d}\xi\\
&\int_{-1}^{1}\left(\frac{\partial w}{\partial y}\right)_{23}\mathrm{d}\eta = d_6 = \int_{-1}^{1}\left(\frac{\partial \tilde{w}}{\partial y}\right)_{23}\mathrm{d}\eta\\
&\int_{-1}^{1}\left(\frac{\partial w}{\partial x}\right)_{43}\mathrm{d}\xi = d_7 = \int_{-1}^{1}\left(\frac{\partial \tilde{w}}{\partial x}\right)_{43}\mathrm{d}\xi\\
&\int_{-1}^{1}w_{12}\mathrm{d}\xi = d_8 = \int_{-1}^{1}\tilde{w}_{12}\mathrm{d}\xi\\
&\int_{-1}^{1}w_{23}\mathrm{d}\eta = d_9 = \int_{-1}^{1}\tilde{w}_{23}\mathrm{d}\eta\\
&\int_{-1}^{1}w_{43}\mathrm{d}\xi = d_{10} = \int_{-1}^{1}\tilde{w}_{43}\mathrm{d}\xi\\
&\left(\frac{\partial w}{\partial x}\right)_1 = d_{11} = \psi_{x1}\\
&\left(\frac{\partial w}{\partial y}\right)_1 = d_{12} = \psi_{y1}
\end{aligned}\right\} \tag{6-24}$$

Equation (6-24) can be written as

$$\hat{\boldsymbol{C}}\boldsymbol{\lambda} = \hat{\boldsymbol{G}}\boldsymbol{q}^e \tag{6-25}$$

where

$$\hat{\boldsymbol{G}}=\begin{bmatrix}
0 & 0 & 1 & 0 & 0 & 1 & 0 & 0 & 0 & 0 & 0 & 0\\
0 & 0 & 0 & 0 & 1 & 0 & 0 & 1 & 0 & 0 & 0 & 0\\
0 & 0 & 0 & 0 & 0 & 0 & 0 & 0 & 1 & 0 & 0 & 1\\
0 & 1 & 0 & 0 & 0 & 0 & 0 & 0 & 0 & 0 & 1 & 0\\
-1 & 0 & 0 & 1 & 0 & 0 & 0 & 0 & 0 & 0 & 0 & 0\\
0 & 0 & 0 & -1 & 0 & 0 & 1 & 0 & 0 & 0 & 0 & 0\\
0 & 0 & 0 & 0 & 0 & 0 & -1 & 0 & 0 & 1 & 0 & 0\\
1 & \frac{a}{3} & 0 & 1 & -\frac{a}{3} & 0 & 0 & 0 & 0 & 0 & 0 & 0\\
0 & 0 & 0 & 1 & 0 & \frac{b}{3} & 1 & 0 & -\frac{b}{3} & 0 & 0 & 0\\
0 & 0 & 0 & 0 & 0 & 0 & 1 & -\frac{a}{3} & 0 & 1 & \frac{a}{3} & 0\\
0 & 1 & 0 & 0 & 0 & 0 & 0 & 0 & 0 & 0 & 0 & 0\\
0 & 0 & 1 & 0 & 0 & 0 & 0 & 0 & 0 & 0 & 0 & 0
\end{bmatrix} \tag{6-26a}$$

$$\hat{\boldsymbol{C}}=\begin{bmatrix}
0 & 0 & \frac{2}{b} & 0 & 0 & -\frac{4}{b} & 0 & \frac{2}{3b} & 0 & \frac{6}{b} & 0 & 0\\
0 & \frac{2}{a} & 0 & \frac{4}{a} & 0 & 0 & \frac{6}{a} & 0 & \frac{2}{3a} & 0 & 0 & 0\\
0 & 0 & \frac{2}{b} & 0 & 0 & \frac{4}{b} & 0 & \frac{2}{3b} & 0 & \frac{6}{b} & 0 & 0\\
0 & \frac{2}{a} & 0 & -\frac{4}{a} & 0 & 0 & \frac{6}{a} & 0 & \frac{2}{3a} & 0 & 0 & 0\\
0 & 2 & 0 & 0 & -2 & 0 & 2 & 0 & 2 & 0 & -2 & -2\\
0 & 0 & 2 & 0 & 2 & 0 & 0 & 2 & 0 & 2 & 2 & 2\\
0 & -2 & 0 & 0 & -2 & 0 & -2 & 0 & -2 & 0 & -2 & -2\\
2 & 0 & -2 & \frac{2}{3} & 0 & 2 & 0 & -\frac{2}{3} & 0 & -2 & 0 & 0\\
2 & 2 & 0 & 2 & 0 & \frac{2}{3} & 2 & 0 & \frac{2}{3} & 0 & 0 & 0\\
2 & 0 & 2 & \frac{2}{3} & 0 & 2 & 0 & \frac{2}{3} & 0 & 2 & 0 & 0\\
0 & \frac{1}{a} & 0 & -\frac{2}{a} & -\frac{1}{a} & 0 & \frac{3}{a} & \frac{2}{a} & \frac{1}{a} & 0 & -\frac{3}{a} & -\frac{1}{a}\\
0 & 0 & \frac{1}{b} & 0 & -\frac{1}{b} & -\frac{2}{b} & 0 & \frac{1}{b} & \frac{2}{b} & \frac{3}{b} & -\frac{1}{b} & -\frac{3}{b}
\end{bmatrix} \tag{6-26b}$$

From Eqs. (6-25) and (6-22), we have

$$w = \boldsymbol{F}_{\lambda}\hat{\boldsymbol{C}}^{-1}\boldsymbol{G}\boldsymbol{q}^{e} \tag{6-27}$$

And then, the element stiffness matrix can be obtained by the conventional procedure.

Example 6.2 Simply-supported and clamped square plates subjected to uniformly distributed load q or central concentrated load P—comparison of different rectangular thin plate elements. L is the length of the plate side; and Poisson's ratio $\mu = 0.3$.

The deflection coefficients at the plate center are given in Table 6.1. For the sake of comparison, not only the results by the generalized conforming element RGC-12 but also those by the element ACM[7] are given (the numbers in parentheses are relative errors). It can be seen from Table 6.1 that the precision of the element RGC-12 is better than that of the element ACM. The moment coefficients are given in Table 6.2, and also exhibit high precision.

Table 6.1 The deflection coefficients at central point

Mesh (whole plate)	Simply-supported			
	α (uniform)		β (concentrated)	
	ACM[7]	RGC-12	ACM[7]	RGC-12
2×2	0.3446(−15%)	0.4003(−1.5%)	1.378(+18.8%)	1.116(−3.8%)
4×4	0.3939(−3%)	0.4034(−0.7%)	1.233(+6.3%)	1.146(−1.2%)
8×8	0.4033(−0.7%)	0.4053(−0.2%)	1.183(+2%)	1.155(−0.4%)
16×16	0.4056(−0.15%)	0.4061(−0.02%)	1.167(+0.6%)	1.159(−0.1%)
Analytical solution	0.4062		1.160	
Mesh (whole plate)	Clamped			
	α (uniform)		β (concentrated)	
	ACM[7]	RGC-12	ACM[7]	RGC-12
2×2	0.1480(+17.0%)	0.1479(+16.9%)	0.5919(+5.5%)	0.5918(+5.5%)
4×4	0.1403(+10.9%)	0.1228(−2.9%)	0.6134(+9.3%)	0.5433(−3.2%)
8×8	0.1304(+3.1%)	0.1253(−0.09%)	0.5803(+3.4%)	0.5550(−1.1%)
16×16	0.1275(+0.08%)	0.1262(−0.02%)	0.5672(+1.1%)	0.5596(−0.3%)
Analytical solution	0.1265		0.5612	

Note: $\begin{cases} w_{\max} = \alpha \dfrac{qL^4}{D}\left(\dfrac{1}{100}\right) & \text{(uniform)} \\ w_{\max} = \beta \dfrac{PL^2}{D}\left(\dfrac{1}{100}\right) & \text{(comcentrated)} \end{cases}$, $D = \dfrac{Eh^3}{12(1-\mu^2)}$, E is the Young's modulus, μ is the Poissom's ratio.

Table 6.2 Moment coefficients

Mesh (whole plate)	Central moment		Moment at mid point of boundary	
	Simply-supported	Clamped	Clamped	
	α_1 (load q)	α_1(load q)	α_1 (load q)	β_1 (load P)
2×2	0.0521(+8.8%)	0.0462(+102%)	−0.0355(+30.8%)	−0.1420(−13.0%)
4×4	0.0484(+1.0%)	0.0239(+4.4%)	−0.0438(+14.6%)	−0.1156(+8.0%)
8×8	0.0479(0%)	0.0230(+0.4%)	−0.0489(+4.7%)	−0.1221(+2.9%)
16×16	0.0479(0%)	0.0230(+0.4%)	−0.0506(+1.4%)	−0.1245(1.0%)
Analytical solution	0.0479	0.0229	−0.0513	−0.1257

Note: $\begin{cases} M=\alpha_1 qL^2 & \text{(uniform)} \\ M=\beta_1 P & \text{(concentrated)} \end{cases}$

6.2.2 Utilization of the Symmetry of Rectangular Elements

We consider the case $m=n=12$ for the rectangular thin plate elements, and take the element RGC-12 as an example. The main construction procedure is how to establish 12 generalized conforming conditions, i.e. Eq. (6-25), in which $\hat{\boldsymbol{C}}$ is a 12×12 matrix. When solving $\boldsymbol{\lambda}$, the inverse matrix $\hat{\boldsymbol{C}}^{-1}$ is needed. It is not an easy work to obtain the inverse matrix of a 12×12 matrix. So, for simplification, the symmetry of the rectangular elements may be used.

In a rectangular element, there are two symmetry axes, that is, x-axis and y-axis in Fig. 6.11. If the symmetry is fully used, the 12 generalized conforming conditions can be classified into four equation groups:

- Symmetry-Symmetry (SS) group—symmetry with respect to both x-axis and y-axis;
- Symmetry-Antisymmetry (SA) group—symmetry with respect to the x-axis, antisymmetry with respect to the y-axis;
- Antisymmetry-Symmetry (AS) group—antisymmetry with respect to the x-axis, symmetry with respect to the y-axis;
- Antisymmetry-Antisymmetry (AA) group—antisymmetry with respect to both x-axis and y-axis.

Thus, each conforming equation group is usually a set of equations with only three unknown variables, which is much simpler to be solved.

Now, let us take the element RGC-12 as an example to illustrate the whole procedure.

Firstly, the element deflection field is expressed by Eqs. (6-22) and (6-23), in which 12 unknown coefficients and their basis functions have already been classified into four groups:

$$\left.\begin{array}{l}\text{SS group}—\lambda_1,\ \lambda_4\xi^2,\ \lambda_6\eta^2\\ \text{SA group}—\lambda_2\xi,\ \lambda_7\xi^3,\ \lambda_9\xi\eta^2\\ \text{AS group}—\lambda_3\eta,\ \lambda_8\xi^2\eta,\ \lambda_{10}\eta^3\\ \text{AA group}—\lambda_5\xi\eta,\ \lambda_{11}\xi^3\eta,\ \lambda_{12}\xi\eta^3\end{array}\right\} \tag{6-28}$$

Secondly, the selected generalized conforming conditions should also possess symmetry or antisymmetry. In fact, all the average line conforming and point conforming conditions about w, ψ_x and ψ_y in Eq. (6-24) do not satisfy this requirement. Therefore, the conforming conditions should be recombined so that the new combination conditions should possess symmetry and antisymmetry, and then, can be vested in one of the above four groups.

For instance, the average line conforming conditions of the rectangular elements can be treated as follows.

In a rectangular element, there are 12 average line conforming conditions about w, ψ_n, ψ_s of each side (the number of independent conditions will be discussed later). According to symmetry or antisymmetry, these conditions can be re-combined to form 12 new combination conditions which are classified as:

(1) Combination conditions belonging to SS group (4 conditions)

$$\int_{-1}^{1}(w_{43}+w_{12})\mathrm{d}\xi=\int_{-1}^{1}(\tilde{w}_{43}+\tilde{w}_{12})\mathrm{d}\xi \tag{6-A1}$$

$$\int_{-1}^{1}(w_{23}+w_{14})\mathrm{d}\eta=\int_{-1}^{1}(\tilde{w}_{23}+\tilde{w}_{14})\mathrm{d}\eta \tag{6-A2}$$

$$\int_{-1}^{1}\left[\left(\frac{\partial w}{\partial x}\right)_{23}-\left(\frac{\partial w}{\partial x}\right)_{14}\right]\mathrm{d}\eta=\int_{-1}^{1}(\tilde{\psi}_{n23}+\tilde{\psi}_{n14})\mathrm{d}\eta \tag{6-A3}$$

$$\int_{-1}^{1}\left[\left(\frac{\partial w}{\partial y}\right)_{43}-\left(\frac{\partial w}{\partial y}\right)_{12}\right]\mathrm{d}\xi=\int_{-1}^{1}(\tilde{\psi}_{n43}+\tilde{\psi}_{n12})\mathrm{d}\xi \tag{6-A4}$$

(2) Combination conditions belonging to SA group (3 conditions)

$$\int_{-1}^{1}(w_{23}-w_{14})\mathrm{d}\eta=\int_{-1}^{1}(\tilde{w}_{23}-\tilde{w}_{14})\mathrm{d}\eta \tag{6-B1}$$

$$\int_{-1}^{1}\left[\left(\frac{\partial w}{\partial x}\right)_{23}+\left(\frac{\partial w}{\partial x}\right)_{14}\right]\mathrm{d}\eta=\int_{-1}^{1}(\tilde{\psi}_{n23}-\tilde{\psi}_{n14})\mathrm{d}\eta \tag{6-B2}$$

$$\int_{-1}^{1}\left[\left(\frac{\partial w}{\partial x}\right)_{43}+\left(\frac{\partial w}{\partial x}\right)_{12}\right]\mathrm{d}\xi=\int_{-1}^{1}(-\tilde{\psi}_{s43}+\tilde{\psi}_{s12})\mathrm{d}\xi \tag{6-B3}$$

(3) Combination conditions belonging to AS group (3 conditions)

$$\int_{-1}^{1}(w_{43}-w_{12})\mathrm{d}\xi=\int_{-1}^{1}(\tilde{w}_{43}-\tilde{w}_{12})\mathrm{d}\xi \tag{6-C1}$$

$$\int_{-1}^{1}\left[\left(\frac{\partial w}{\partial y}\right)_{43}+\left(\frac{\partial w}{\partial y}\right)_{12}\right]\mathrm{d}\xi=\int_{-1}^{1}(\tilde{\psi}_{n43}-\tilde{\psi}_{n12})\mathrm{d}\xi \tag{6-C2}$$

$$\int_{-1}^{1}\left[\left(\frac{\partial w}{\partial y}\right)_{23}+\left(\frac{\partial w}{\partial y}\right)_{14}\right]\mathrm{d}\eta=\int_{-1}^{1}(\tilde{\psi}_{s23}-\tilde{\psi}_{s14})\mathrm{d}\eta \tag{6-C3}$$

(4) Combination conditions belonging to AA group (2 conditions)

$$\int_{-1}^{1}\left[\left(\frac{\partial w}{\partial x}\right)_{43}-\left(\frac{\partial w}{\partial x}\right)_{12}\right]\mathrm{d}\xi=\int_{-1}^{1}-(\tilde{\psi}_{s43}+\tilde{\psi}_{s12})\mathrm{d}\xi \tag{6-D1}$$

$$\int_{-1}^{1}\left[\left(\frac{\partial w}{\partial y}\right)_{23}-\left(\frac{\partial w}{\partial y}\right)_{14}\right]\mathrm{d}\eta=\int_{-1}^{1}(\tilde{\psi}_{s23}+\tilde{\psi}_{s14})\mathrm{d}\eta \tag{6-D2}$$

The combination conforming conditions are derived by selecting the combination boundary forces as weighting functions. The above conforming condition groups are just classified by the symmetry or antisymmetry of the selected combination boundary forces.

Substitution of the element deflection field (6-22) and the interpolation formulae for boundary displacements into the above 12 conditions yields

(1) SS group

$$\lambda_1+\frac{1}{3}\lambda_4+\lambda_6=\frac{1}{4}\sum_{i=1}^{4}w_i-\frac{a}{12}\sum_{i=1}^{4}\psi_{xi}\xi_i \tag{6-A1)′}$$

$$\lambda_1+\lambda_4+\frac{1}{3}\lambda_6=\frac{1}{4}\sum_{i=1}^{4}w_i-\frac{b}{12}\sum_{i=1}^{4}\psi_{yi}\eta_i \tag{6-A2)′}$$

$$\lambda_4=\frac{a}{8}\sum_{i=1}^{4}\psi_{xi}\xi_i \tag{6-A3)′}$$

$$\lambda_6=\frac{b}{8}\sum_{i=1}^{4}\psi_{yi}\eta_i \tag{6-A4)′}$$

(2) SA group

$$\lambda_2 + \lambda_7 + \frac{1}{3}\lambda_9 = \frac{1}{4}\sum_{i=1}^{4} w_i\xi_i - \frac{b}{12}\sum_{i=1}^{4}\psi_{yi}\xi_i\eta_i \tag{6-B1)'}$$

$$\lambda_2 + 3\lambda_7 + \frac{1}{3}\lambda_9 = \frac{a}{4}\sum_{i=1}^{4}\psi_{xi} \tag{6-B2)'}$$

$$\lambda_2 + \lambda_7 + \lambda_9 = \frac{1}{4}\sum_{i=1}^{4} w_i\xi_i \tag{6-B3)'}$$

(3) AS group

$$\lambda_3 + \frac{1}{3}\lambda_8 + \lambda_{10} = \frac{1}{4}\sum_{i=1}^{4} w_i\eta_i - \frac{a}{12}\sum_{i=1}^{4}\psi_{xi}\xi_i\eta_i \tag{6-C1)'}$$

$$\lambda_3 + \frac{1}{3}\lambda_8 + 3\lambda_{10} = \frac{b}{4}\sum_{i=1}^{4}\psi_{yi} \tag{6-C2)'}$$

$$\lambda_3 + \lambda_8 + \lambda_{10} = \frac{1}{4}\sum_{i=1}^{4} w_i\eta_i \tag{6-C3)'}$$

(4) AA group

$$\lambda_5 + \lambda_{11} + \lambda_{12} = \frac{1}{4}\sum_{i=1}^{4} w_i\xi_i\eta_i \tag{6-D1)'}$$

$$\lambda_5 + \lambda_{11} + \lambda_{12} = \frac{1}{4}\sum_{i=1}^{4} w_i\xi_i\eta_i \tag{6-D2)'}$$

There are total 12 equations above, in which only 10 are independent, that is, 2 equations are not independent.

Firstly, the two Eqs. (6-D1)′ and (6-D2)′ in the AA group are actually the same, so one of these two conditions is not independent. This is an inevitable result produced by the identical Eq. (6-4), which shows that four average line conforming conditions about ψ_s along four element sides should contain an independent one.

Secondly, there is an independent equation among the four Eqs. (6-A1)′, (6-A2)′, (6-A3)′ and (6-A4)′ in the SS group. For example, Eq. (6-A2)′ can be derived from the other three equations. This is because only three unknown coefficients (λ_1, λ_2, λ_3) are involved in the four equations of the SS group. If it is not a contradictory equation set, it must contain an independent equation.

Anyway, we have only 10 independent conditions here. The first three groups separately have three independent equations, from which three unknown coefficients of each group can be solved.

SS group

$$\left.\begin{aligned}\lambda_1 &= \frac{1}{4}\sum_{i=1}^{4} w_i - \frac{a}{8}\sum_{i=1}^{4}\psi_{xi}\xi_i - \frac{b}{8}\sum_{i=1}^{4}\psi_{yi}\eta_i \\ \lambda_4 &= \frac{a}{8}\sum_{i=1}^{4}\psi_{xi}\xi_i \\ \lambda_6 &= \frac{b}{8}\sum_{i=1}^{4}\psi_{yi}\eta_i\end{aligned}\right\} \tag{6-29}$$

SA group

$$\left.\begin{aligned}\lambda_2 &= \frac{3}{8}\sum_{i=1}^{4} w_i\xi_i - \frac{a}{8}\sum_{i=1}^{4}\psi_{xi} - \frac{b}{6}\sum_{i=1}^{4}\psi_{yi}\xi_i\eta_i \\ \lambda_7 &= -\frac{1}{8}\sum_{i=1}^{4} w_i\xi_i + \frac{a}{8}\sum_{i=1}^{4}\psi_{xi} + \frac{b}{24}\sum_{i=1}^{4}\psi_{yi}\xi_i\eta_i \\ \lambda_9 &= \frac{b}{8}\sum_{i=1}^{4}\psi_{yi}\xi_i\eta_i\end{aligned}\right\} \tag{6-30}$$

AS group

$$\left.\begin{aligned}\lambda_3 &= \frac{3}{8}\sum_{i=1}^{4} w_i\eta_i - \frac{a}{6}\sum_{i=1}^{4}\psi_{xi}\xi_i\eta_i - \frac{b}{8}\sum_{i=1}^{4}\psi_{yi} \\ \lambda_8 &= \frac{a}{8}\sum_{i=1}^{4}\psi_{xi}\xi_i\eta_i \\ \lambda_{10} &= -\frac{1}{8}\sum_{i=1}^{4} w_i\eta_i + \frac{a}{24}\sum_{i=1}^{4}\psi_{xi}\xi_i\eta_i + \frac{b}{8}\sum_{i=1}^{4}\psi_{yi}\end{aligned}\right\} \tag{6-31}$$

As for the AA group, there is only one independent condition (6-D1)′. So, two conforming conditions should be supplemented for solving the three unknown coefficients λ_5, λ_{11}, λ_{12}.

In the element RGC-12, the two supplementary conditions are the last two point conforming conditions,

$$\left(\frac{\partial w}{\partial x}\right)_1 = \psi_{x1}, \quad \left(\frac{\partial w}{\partial y}\right)_1 = \psi_{y1}$$

that is

$$\begin{aligned}-2\lambda_4 + (\lambda_2 + 3\lambda_7 + \lambda_9) + 2\lambda_8 - (\lambda_5 + 3\lambda_{11} + \lambda_{12}) &= a\psi_{x1} \\ -2\lambda_6 + 2\lambda_9 + (\lambda_3 + \lambda_8 + 3\lambda_{10}) - (\lambda_5 + \lambda_{11} + 3\lambda_{12}) &= b\psi_{y1}\end{aligned}$$

Solving the simultaneous equations of the above two equations and Eq. (6-D1)′, the

remaining three unknown coefficients can be obtained:

$$\left.\begin{aligned}
\lambda_5 &= \frac{1}{2}\sum_{i=1}^{4} w_i\xi_i\eta_i - \frac{a}{8}\sum_{i=1}^{4}\psi_{xi}\left(1+\frac{1}{3}\xi_i\right)\eta_i - \frac{b}{8}\sum_{i=1}^{4}\psi_{yi}\xi_i\left(1+\frac{1}{3}\eta_i\right)\\
\lambda_{11} &= -\frac{1}{8}\sum_{i=1}^{4} w_i\xi_i\eta_i + \frac{a}{8}\sum_{i=1}^{4}\psi_{xi}\eta_i + \frac{b}{24}\sum_{i=1}^{4}\psi_{yi}\xi_i\eta_i\\
\lambda_{12} &= -\frac{1}{8}\sum_{i=1}^{4} w_i\xi_i\eta_i + \frac{a}{24}\sum_{i=1}^{4}\psi_{xi}\xi_i\eta_i + \frac{b}{8}\sum_{i=1}^{4}\psi_{yi}\xi_i
\end{aligned}\right\} \tag{6-32}$$

Though the above two supplementary conditions are simple and feasible, they are related to the numbering of the element nodes. So, the following two combination point conforming conditions are more reasonable (belong to the AA group):

$$\left.\begin{aligned}
\sum_{i=1}^{4}\left(\frac{\partial w}{\partial x}\right)_i \eta_i &= \sum_{i=1}^{4}\psi_{xi}\eta_i\\
\sum_{i=1}^{4}\left(\frac{\partial w}{\partial y}\right)_i \xi_i &= \sum_{i=1}^{4}\psi_{yi}\xi_i
\end{aligned}\right\} \tag{6-33}$$

that is

$$\left.\begin{aligned}
\lambda_5 + 3\lambda_{11} + \lambda_{12} &= \frac{a}{4}\sum_{i=1}^{4}\psi_{xi}\eta_i\\
\lambda_5 + \lambda_{11} + 3\lambda_{12} &= \frac{b}{4}\sum_{i=1}^{4}\psi_{yi}\xi_i
\end{aligned}\right\} \tag{6-34}$$

Solving Eqs. (6-34) and (6-D1)′ simultaneously, we obtain

$$\left.\begin{aligned}
\lambda_5 &= \frac{1}{2}\sum_{i=1}^{4} w_i\xi_i\eta_i - \frac{a}{8}\sum_{i=1}^{4}\psi_{xi}\eta_i - \frac{b}{8}\sum_{i=1}^{4}\psi_{yi}\xi_i\\
\lambda_{11} &= -\frac{1}{8}\sum_{i=1}^{4} w_i\xi_i\eta_i + \frac{a}{8}\sum_{i=1}^{4}\psi_{xi}\eta_i\\
\lambda_{12} &= -\frac{1}{8}\sum_{i=1}^{4} w_i\xi_i\eta_i + \frac{b}{8}\sum_{i=1}^{4}\psi_{yi}\xi_i
\end{aligned}\right\} \tag{6-35}$$

The element obtained by this scheme is the same as no. 23 element LR12-2 in Table 5.1, only the derivation procedures are different.

6.2.3 Rectangular Element RGC-12 (Buckling Problem)

Now, consider the buckling problem for thin plates. The in-plane stress resultants N_x, N_y and N_{xy} of the mid-plane are assumed to be linearly distributed (as shown

in Fig. 6.12):

$$\left.\begin{aligned} N_x &= -(P_x + \xi Q_x + \eta R_x) \\ N_y &= -(P_y + \xi Q_y + \eta R_y) \\ N_{xy} &= -(P_{xy} + \xi Q_{xy} + \eta R_{xy}) \end{aligned}\right\} \tag{6-36}$$

where P_x, P_y, P_{xy}, Q_x, Q_y, Q_{xy}, R_x, R_y, R_{xy} are all constants.

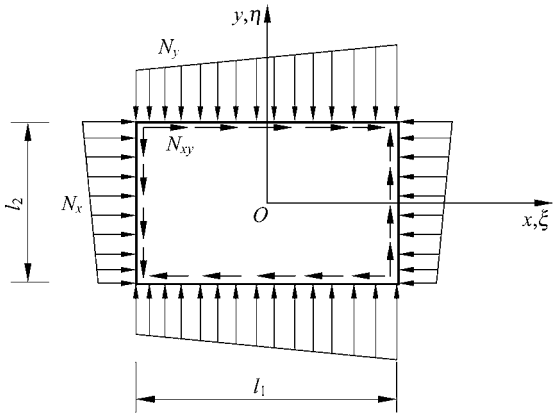

Figure 6.12 Stability problem for thin plates

The geometric stiffness matrix of the generalized conforming element is given by

$$\boldsymbol{g}^e = (\hat{\boldsymbol{C}}^{-1}\hat{\boldsymbol{G}})^{\mathrm{T}}\, \boldsymbol{g}_{\lambda\lambda}{}^e (\hat{\boldsymbol{C}}^{-1}\hat{\boldsymbol{G}}) \tag{6-37}$$

where

$$\begin{aligned} \boldsymbol{g}_{\lambda\lambda}{}^e = \int_{-1}^{1}\int_{-1}^{1} \Big\{ & \frac{b}{a}(P_x + \xi Q_x + \eta R_x)\boldsymbol{F}_{\lambda,\xi}{}^{\mathrm{T}}\boldsymbol{F}_{\lambda,\xi} + \frac{a}{b}(P_y + \xi Q_y + \eta R_y)\boldsymbol{F}_{\lambda,\eta}{}^{\mathrm{T}}\boldsymbol{F}_{\lambda,\eta} \\ & + (P_{xy} + \xi Q_{xy} + \eta R_{xy})(\boldsymbol{F}_{\lambda,\xi}{}^{\mathrm{T}}\boldsymbol{F}_{\lambda,\eta} + \boldsymbol{F}_{\lambda,\eta}{}^{\mathrm{T}}\boldsymbol{F}_{\lambda,\xi}) \Big\} \mathrm{d}\xi \mathrm{d}\eta \end{aligned} \tag{6-38}$$

in which $\boldsymbol{F}_{\lambda,\xi}$ and $\boldsymbol{F}_{\lambda,\eta}$ denote the derivatives of $\boldsymbol{F}_\lambda$ with respect to ξ and η, respectively.

Then the critical load of the thin plate can be calculated by the above stiffness matrix $\boldsymbol{K}^e$ and geometric stiffness matrix $\boldsymbol{g}^e$ of the generalized conforming element.

Example 6.3 The buckling critical load $P_{x\mathrm{cr}}$ for the simply-supported and clamped square plates subjected to uniform compression in one direction. The length of the plate side is L.

The results of the buckling critical load $P_{x\mathrm{cr}}$ calculated from the element RGC-12 are given in Table 6.3. Compared with the results given by reference [8], this generalized conforming element gives more accurate results. The numbers in parentheses are relative errors.

Table 6.3 Coefficient k for square plate under compression in one direction

Mesh (whole plate)	Simply-supported		Clamped	
	Kapur [8]	RGC-12	Kapur [8]	RGC-12
4×4	3.770(−5.8%)	4.128(+3.2%)	9.28(−7.8%)	9.70(−3.7%)
6×6	3.887(−2.8%)	4.028(+0.7%)	9.61(−4.6%)	10.12(+0.5%)
8×8	3.933(−1.7%)	4.009(+0.2%)	9.78(−2.9%)	10.12(+0.5%)
10×10	3.960(−1.0%)	4.002(+0.05%)	9.89(−1.8%)	10.12(+0.5%)
Analytical solution	4.000		10.07	

Note: $P_{x\mathrm{cr}}=k\dfrac{\pi^2D}{l^2}$

Example 6.4 The buckling critical load $P_{xy\mathrm{cr}}$ for a simply-supported rectangular plate $\left(\dfrac{L_1}{L_2}=1.25\right)$ under shear load.

The results are given in Table 6.4. Compared with those given in reference [8], the generalized conforming element gives more accurate results.

Table 6.4 Coefficient k for a simply-supported rectangular plate $\left(\dfrac{L_1}{L_2}=\dfrac{5}{4}\right)$ under shear load

Mesh (whole plate)	Kapur[8]	RGC-12
4×4	6.95(−9.9%)	7.84(+1.7%)
6×6	7.25(−6.0%)	7.74(+0.4%)
8×8	7.45(−3.4%)	7.74(+0.4%)
10×10	—	7.72(+0.1%)
Analytical solution	7.71	

Note: $P_{xy\mathrm{cr}}=k\dfrac{\pi^2D}{l_2^2}$

6.2.4 Rectangular Element CGC-R12[9]

The element CGC-R12 is also a rectangular thin plate element with 12 DOFs, which are still the deflection w_i, rotations ψ_{xi} and ψ_{yi} ($i=1, 2, 3, 4$) at each corner node.

The element deflection field is assumed to be an incomplete quartic polynomial containing 12 unknown coefficients, and expressed in terms of the dimensionless rectangular coordinates ξ and η as follows:

$$\begin{aligned} w = {} & \lambda_1 + \lambda_2\xi + \lambda_3\eta + \lambda_4\xi\eta + (\xi^2 - 1)(\lambda_5 + \lambda_7\eta + \lambda_9\xi) \\ & + (\eta^2 - 1)(\lambda_6 + \lambda_8\xi + \lambda_{10}\eta) + \lambda_{11}(\xi^4 - 1) + \lambda_{12}(\eta^4 - 1) \end{aligned} \tag{6-39}$$

According to the line-point conforming scheme, 12 conforming conditions are selected as follows:

(1) point conforming conditions of w at the corner nodes (4 conditions)

$$w_i - \tilde{w}_i = 0 \quad (i = 1,2,3,4) \tag{6-40}$$

(2) average line conforming conditions of w and ψ_n along the element sides (8 conditions)

$$\int_{d_{ij}} (w - \tilde{w})\mathrm{d}s = 0 \quad (ij = 12,23,34,41) \tag{6-41}$$

$$\int_{d_{ij}} \left(\frac{\partial w}{\partial n} - \tilde{\psi}_n \right) \mathrm{d}s = 0 \quad (ij = 12,23,34,41) \tag{6-42}$$

From the four point conforming conditions in Eq. (6-40), the first four unknown coefficients can be obtained:

$$\lambda_1 = \frac{1}{4}\sum_{i=1}^{4} w_i\,, \quad \lambda_2 = \frac{1}{4}\sum_{i=1}^{4} w_i\xi_i\,, \quad \lambda_3 = \frac{1}{4}\sum_{i=1}^{4} w_i\eta_i\,, \quad \lambda_4 = \frac{1}{4}\sum_{i=1}^{4} w_i\xi_i\eta_i \tag{6-43}$$

Substitution of the above equation into Eq. (6-39) yields

$$\begin{aligned} w = {} & \frac{1}{4}\sum_{i=1}^{4} w_i(1 + \xi_i\xi)(1 + \eta_i\eta) + (\xi^2 - 1)(\lambda_5 + \lambda_7\eta + \lambda_9\xi) \\ & + (\eta^2 - 1)(\lambda_6 + \lambda_8\xi + \lambda_{10}\eta) + \lambda_{11}(\xi^4 - 1) + \lambda_{12}(\eta^4 - 1) \end{aligned} \tag{6-44}$$

And, the residual eight unknown coefficients can be determined by the line conforming conditions (6-41) and (6-42). For simplification, the combination conforming conditions with symmetry or antisymmetry can be used again.

Firstly, in Eq. (6-44), four unknown coefficients λ_5, λ_6, λ_{11} and λ_{12} belong to the SS group; two unknown coefficients λ_8 and λ_9 belong to the SA group; and two unknown coefficients λ_7 and λ_{10} belong to the AS group.

Secondly, eight combination conditions can be formed from Eqs. (6-41) and (6-42), in which four conditions (6-A1), (6-A2), (6-A3) and (6-A4) of the SS group can just be used to solve λ_5, λ_6, λ_{11} and λ_{12}; two conditions (6-B1) and

(6-B2) of the SA group can just be used to solve λ_8 and λ_9; and two conditions (6-C1) and (6-C2) of the AS group can just be used to solve λ_7 and λ_{10}. After substituting the deflection field (6-44) and the interpolation formulae for boundary, equations of these three groups can be written as:

SS group

$$\left.\begin{aligned}
&\sum_{i=1}^{4} w_i - \frac{8}{3}\lambda_5 - \frac{16}{5}\lambda_{11} = \sum_{i=1}^{4} w_i - \frac{a}{3}\sum_{i=1}^{4}\psi_{xi}\xi_i \\
&\sum_{i=1}^{4} w_i - \frac{8}{3}\lambda_6 - \frac{16}{5}\lambda_{12} = \sum_{i=1}^{4} w_i - \frac{b}{3}\sum_{i=1}^{4}\psi_{yi}\eta_i \\
&\frac{8}{a}(\lambda_5 + 2\lambda_{11}) = \sum_{i=1}^{4}\psi_{xi}\xi_i \\
&\frac{8}{b}(\lambda_6 + 2\lambda_{12}) = \sum_{i=1}^{4}\psi_{yi}\eta_i
\end{aligned}\right\} \tag{6-45}$$

SA group

$$\left.\begin{aligned}
&\sum_{i=1}^{4} w_i\xi_i - \frac{8}{3}\lambda_8 = \sum_{i=1}^{4} w_i\xi_i - \frac{b}{3}\sum_{i=1}^{4}\psi_{yi}\xi_i\eta_i \\
&\frac{1}{a}\sum_{i=1}^{4} w_i\xi_i + \frac{8}{a}\lambda_9 - \frac{8}{3a}\lambda_8 = \sum_{i=1}^{4}\psi_{xi}
\end{aligned}\right\} \tag{6-46}$$

AS group

$$\left.\begin{aligned}
&\sum_{i=1}^{4} w_i\eta_i - \frac{8}{3}\lambda_7 = \sum_{i=1}^{4} w_i\eta_i - \frac{a}{3}\sum_{i=1}^{4}\psi_{xi}\xi_i\eta_i \\
&\frac{1}{b}\sum_{i=1}^{4} w_i\eta_i - \frac{8}{3b}\lambda_7 + \frac{8}{b}\lambda_{10} = \sum_{i=1}^{4}\psi_{yi}
\end{aligned}\right\} \tag{6-47}$$

Thus, we can obtain

$$\left.\begin{aligned}
&\lambda_5 = \frac{a}{8}\sum_{i=1}^{4}\psi_{xi}\xi_i, \quad \lambda_6 = \frac{b}{8}\sum_{i=1}^{4}\psi_{yi}\eta_i, \quad \lambda_{11} = 0, \quad \lambda_{12} = 0 \\
&\lambda_8 = \frac{b}{8}\sum_{i=1}^{4}\psi_{yi}\xi_i\eta_i, \quad \lambda_9 = -\frac{1}{8}\sum_{i=1}^{4} w_i\xi_i + \frac{a}{8}\sum_{i=1}^{4}\psi_{xi} + \frac{b}{24}\sum_{i=1}^{4}\psi_{yi}\xi_i\eta_i \\
&\lambda_7 = \frac{a}{8}\sum_{i=1}^{4}\psi_{xi}\xi_i\eta_i, \quad \lambda_{10} = -\frac{1}{8}\sum_{i=1}^{4} w_i\eta_i + \frac{a}{24}\sum_{i=1}^{4}\psi_{xi}\xi_i\eta_i + \frac{b}{8}\sum_{i=1}^{4}\psi_{yi}
\end{aligned}\right\} \tag{6-48}$$

Substitution of Eqs. (6-48) into (6-44) yields

$$w = \sum_{i=1}^{4}(N_i w_i + N_{xi}\psi_{xi} + N_{yi}\psi_{yi}) \tag{6-49}$$

where N_i, N_{xi} and N_{yi} are shape functions

$$\left.\begin{aligned} N_i &= \frac{1}{8}[2(1+\xi_i\xi)(1+\eta_i\eta)-\xi_i\xi(\xi^2-1)-\eta_i\eta(\eta^2-1)] \\ N_{xi} &= \frac{a\xi_i}{24}[3(1+\xi_i\xi+\eta_i\eta)(\xi^2-1)+\eta_i\eta(\eta^2-1)] \\ N_{yi} &= \frac{b\eta_i}{24}[3(1+\xi_i\xi+\eta_i\eta)(\eta^2-1)+\xi_i\xi(\xi^2-1)] \end{aligned}\right\} \tag{6-50}$$

Then, the element stiffness matrix can be obtained by the conventional procedure.

Example 6.5 The central deflection and moment of the simply-supported and clamped square plates subjected to vertical uniformly distributed load q and concentrated load P.

Table 6.5 The central deflection and moment of plates subjected to uniform load

	Central deflection w				Central moment M			
	Simply-supported		Clamped		Simply-supported		Clamped	
Elements	ACM	CGC-R12	ACM	CGC-R12	ACM	CGC-R12	ACM	CGC-R12
2×2	0.432 82	0.405 23	0.140 33	0.124 47	0.521 69	0.510 60	0.277 83	0.271 16
4×4	0.412 94	0.406 16	0.133 23	0.126 26	0.489 20	0.487 72	0.240 50	0.240 69
6×6	0.409 21	0.406 22	0.128 28	0.126 47	0.483 42	0.482 72	0.234 09	0.234 43
8×8	0.408 09	0.406 23	0.127 54	0.126 51	0.481 66	0.481 01	0.231 91	0.232 13
Analytical	0.406 24$qL^4/(100D)$		0.126 53$qL^4/(100D)$		0.478 86$qL^2/10$		0.229 05$qL^2/10$	

Table 6.6 The central deflection of plates subjected to concentrated load

	Simply-supported		Clamped	
Elements	ACM	CGC-R12	ACM	CGC-R12
2×2	0.123 27	0.118 71	0.613 45	0.580 62
4×4	0.118 29	0.116 89	0.580 26	0.568 89
6×6	0.117 14	0.116 42	0.570 99	0.565 03
8×8	0.116 74	0.116 24	0.567 30	0.563 44
Analytical	0.1160$PL^2/(10D)$		0.5612$PL^2/(100D)$	

The length of the plate side is L, and Poisson's ratio is 0.3.

Due to symmetry, only one quarter of the plate is meshed. Results by the elements CGC-R12 and ACM are listed in Tables 6.5 and 6.6.

6.3 Line-Point Conforming Scheme—Triangular Elements

This section will introduce the triangular thin plate elements ($m = n = 9$) constructed by the combination scheme of line conforming and point conforming. The no. 6, 7, 8 and 9 elements LZ1, LZ2, GPL-T9 and GCIV-T9 in Table 5.1 all belong to this element group.

6.3.1 Triangular Element LZ1[10]

A triangular thin plate bending element with 9 DOFs is shown in Fig. 6.1. The nodal displacement vector $\boldsymbol{q}^e$ is

$$\boldsymbol{q}^e = [w_1 \quad \psi_{x1} \quad \psi_{y1} \quad w_2 \quad \psi_{x2} \quad \psi_{y2} \quad w_3 \quad \psi_{x3} \quad \psi_{y3}]^{\mathrm{T}}$$

The displacements along each element side are interpolated by $\boldsymbol{q}^e$, i.e., along each element side, the deflection $\tilde{w}$ is assumed to be cubic and the normal slope $\tilde{\psi}_n$ linearly distributed.

The element deflection field is assumed to be an incomplete cubic polynomial with 9 unknown coefficients, and expressible in terms of the area coordinates L_1, L_2, L_3 as

$$w = \boldsymbol{F}_\lambda \boldsymbol{\lambda} \tag{6-51}$$

where $\boldsymbol{\lambda}$ contains 9 unknown coefficients

$$\boldsymbol{\lambda} = [\lambda_1 \quad \lambda_2 \quad \cdots \quad \lambda_9]^{\mathrm{T}}$$

$\boldsymbol{F}_\lambda$ contains 9 basis functions

$$\boldsymbol{F}_\lambda = [L_1 \quad L_2 \quad L_3 \quad L_1L_2 \quad L_2L_3 \quad L_3L_1 \quad L_1^2L_2 \quad L_2^2L_3 \quad L_3^2L_1] \tag{6-52}$$

In order to solve the 9 unknown coefficients in terms of $\boldsymbol{q}^e$, according to the line-point conforming combination scheme, 9 conforming conditions can be selected as follows:

$$(w - \tilde{w})_j = 0 \quad (j=1, 2, 3) \tag{6-53}$$

$$\int_{S_k} (w - \tilde{w})\mathrm{d}s = 0, \quad \int_{S_k} \left(\frac{\partial w}{\partial n} - \tilde{\psi}_n \right) \mathrm{d}s = 0 \quad (k = 1,2,3) \tag{6-54}$$

Equation (6-53) denotes the point conforming conditions at three corner nodes; Eq. (6-54) denotes the average line conforming conditions of deflections and rotations along three sides.

From Eq. (6-53), the first three unknown coefficients can be obtained

$$\lambda_1 = w_1, \quad \lambda_2 = w_2, \quad \lambda_3 = w_3 \tag{6-55}$$

From Eq. (6-54), the following six equations can be obtained

$$\left.\begin{aligned} 2\lambda_4 + \lambda_7 &= c_3(\psi_{x1} - \psi_{x2}) - b_3(\psi_{y1} - \psi_{y2}) \\ 2\lambda_5 + \lambda_8 &= c_1(\psi_{x2} - \psi_{x3}) - b_1(\psi_{y2} - \psi_{y3}) \\ 2\lambda_6 + \lambda_9 &= c_2(\psi_{x3} - \psi_{x1}) - b_2(\psi_{y3} - \psi_{y1}) \end{aligned}\right\} \tag{6-56}$$

$$\left.\begin{aligned} \lambda_4 - \lambda_5 - \lambda_6 + \frac{2}{3}\lambda_7 - \frac{2}{3}\lambda_8 &= -(1+r_3)w_1 - (1-r_3)w_2 + 2w_3 \\ &\quad - \frac{2A}{d_3^2}[b_3(\psi_{x1} + \psi_{x2}) + c_3(\psi_{y1} + \psi_{y2})] \\ -\lambda_4 + \lambda_5 - \lambda_6 + \frac{2}{3}\lambda_8 - \frac{2}{3}\lambda_9 &= 2w_1 - (1+r_1)w_2 - (1-r_1)w_3 \\ &\quad - \frac{2A}{d_1^2}[b_1(\psi_{x2} + \psi_{x3}) + c_1(\psi_{y2} + \psi_{y3})] \\ -\lambda_4 - \lambda_5 + \lambda_6 - \frac{2}{3}\lambda_7 + \frac{2}{3}\lambda_9 &= -(1-r_2)w_1 + 2w_2 - (1+r_2)w_3 \\ &\quad - \frac{2A}{d_2^2}[b_2(\psi_{x3} + \psi_{x1}) + c_2(\psi_{y3} + \psi_{y1})] \end{aligned}\right\} \tag{6-57}$$

where

$$b_i = y_j - y_k, \quad c_i = x_k - x_j, \quad r_i = \frac{d_j^2 - d_k^2}{d_i^2} \quad (i = \overrightarrow{1,2,3}; \quad j = \overrightarrow{2,3,1}; \quad k = \overrightarrow{3,1,2}) \tag{6-58}$$

d_1, d_2, and d_3 denote the side lengths of the element; A is the area of the triangle.

The last six unknown coefficients can be determined from Eqs. (6-56) and (6-57).

Combining the above results, we have

$$\boldsymbol{\lambda} = \hat{\boldsymbol{A}}\boldsymbol{q}^e \tag{6-59}$$

where

$$\hat{\boldsymbol{A}} = [\hat{\boldsymbol{A}}_1 \quad \hat{\boldsymbol{A}}_2 \quad \hat{\boldsymbol{A}}_3] \tag{6-60}$$

with

$$\hat{\boldsymbol{A}}_1 = \begin{bmatrix} 1 & 0 & 0 \\ 0 & 0 & 0 \\ 0 & 0 & 0 \\ -\frac{1}{6}(9-r_2-2r_3) & -\frac{1}{12}(r_2c_2-2r_3c_3-3c_2) & \frac{1}{12}(r_2b_2-2r_3b_3-3b_2) \\ -\frac{1}{6}(5r_2+r_3) & -\frac{1}{12}(-5r_2c_2+r_3c_3+3c_1) & \frac{1}{12}(-5r_2b_2+r_3b_3+3b_1) \\ -\frac{1}{6}(-9+2r_2-5r_3) & -\frac{1}{12}(-2r_2c_2-5r_3c_3+12c_2-3c_3) & \frac{1}{12}(-2r_2b_2-5r_3b_3+12b_2-3b_3) \\ \frac{1}{3}(9-r_2-2r_3) & \frac{1}{6}(r_2c_2-2r_3c_3-3c_2+6c_3) & -\frac{1}{6}(r_2b_2-2r_3b_3-3b_2+6b_3) \\ \frac{1}{3}(5r_2+r_3) & \frac{1}{6}(-5r_2c_2+r_3c_3+3c_1) & -\frac{1}{6}(-5r_2b_2+r_3b_3+3b_1) \\ \frac{1}{3}(-9+2r_2-5r_3) & \frac{1}{6}(-2r_2c_2-5r_3c_3+6c_2-3c_3) & -\frac{1}{6}(-2r_2b_2-5r_3b_3+6b_2-3b_3) \end{bmatrix} \tag{6-61}$$

$$\hat{\boldsymbol{A}}_2 = \begin{bmatrix} 0 & 0 & 0 \\ 1 & 0 & 0 \\ 0 & 0 & 0 \\ -\frac{1}{6}(-9+2r_3-5r_1) & -\frac{1}{12}(-2r_3c_3-5r_1c_1+12c_3-3c_1) & \frac{1}{12}(-2r_3b_3-5r_1b_1+12b_3-3b_1) \\ -\frac{1}{6}(9-r_3-2r_1) & -\frac{1}{12}(r_3c_3-2r_1c_1-3c_3) & \frac{1}{12}(r_3b_3-2r_1b_1-3b_3) \\ -\frac{1}{6}(5r_3+r_1) & -\frac{1}{12}(-5r_3c_3+r_1c_1+3c_2) & \frac{1}{12}(-5r_3b_3+r_1b_1+3b_2) \\ \frac{1}{3}(-9+2r_3-5r_1) & \frac{1}{6}(-2r_3c_3-5r_1c_1+6c_3-3c_1) & -\frac{1}{6}(-2r_3b_3-5r_1b_1+6b_3-3b_1) \\ \frac{1}{3}(9-r_3-2r_1) & \frac{1}{6}(r_3c_3-2r_1c_1-3c_3+6c_1) & -\frac{1}{6}(r_3b_3-2r_1b_1-3b_3+6b_1) \\ \frac{1}{3}(5r_3+r_1) & \frac{1}{6}(-5r_3c_3+r_1c_1+3c_2) & -\frac{1}{6}(-5r_3b_3+r_1b_1+3b_2) \end{bmatrix} \tag{6-62}$$

$$\hat{\boldsymbol{A}}_3=\begin{bmatrix} 0 & 0 & 0 \\ 0 & 0 & 0 \\ 1 & 0 & 0 \\ -\frac{1}{6}(5r_1+r_2) & -\frac{1}{12}(-5r_1c_1+r_2c_2+3c_3) & \frac{1}{12}(-5r_1b_1+r_2b_2+3b_3) \\ -\frac{1}{6}(-9+2r_1-5r_2) & -\frac{1}{12}(-2r_1c_1-5r_2c_2+12c_1-3c_2) & \frac{1}{12}(-2r_1b_1-5r_2b_2+12b_1-3b_2) \\ -\frac{1}{6}(9-r_1-2r_2) & -\frac{1}{12}(r_1c_1-2r_2c_2-3c_1) & \frac{1}{12}(r_1b_1-2r_2b_2-3b_1) \\ \frac{1}{3}(5r_1+r_2) & \frac{1}{6}(-5r_1c_1+r_2c_2+3c_3) & -\frac{1}{6}(-5r_1b_1+r_2b_2+3b_3) \\ \frac{1}{3}(-9+2r_1-5r_2) & \frac{1}{6}(-2r_1c_1-5r_2c_2+6c_1-3c_2) & -\frac{1}{6}(-2r_1b_1-5r_2b_2+6b_1-3b_2) \\ \frac{1}{3}(9-r_1-2r_2) & \frac{1}{6}(r_1c_1-2r_2c_2-3c_1+6c_2) & -\frac{1}{6}(r_1b_1-2r_2b_2-3b_1+6b_2) \end{bmatrix} \tag{6-63}$$

Substituting Eq. (6-59) into Eq. (6-51), we obtain

$$w=\boldsymbol{F}_\lambda\hat{\boldsymbol{A}}\boldsymbol{q}^e \tag{6-64}$$

The element shape function matrix is

$$\boldsymbol{N}=\boldsymbol{F}_\lambda\hat{\boldsymbol{A}} \tag{6-65}$$

Then, the element stiffness matrix $\boldsymbol{K}^e$ can be derived by the conventional procedure.

6.3.2 Triangular Element LZ2[10]

Assume that the element deflection field w consists of two parts,

$$w=w_q+w_\alpha \tag{6-66}$$

where the first part is the deflection field expressed in Eq. (6-64)

$$w_q=\boldsymbol{F}_\lambda\hat{\boldsymbol{A}}\boldsymbol{q}^e$$

and the second part is a generalized bubble deflection field

$$w_\alpha=F_\alpha\alpha \tag{6-67}$$

in which α is an internal displacement parameter and F_α is a generalized bubble function

$$F_\alpha=-(L_1L_2+L_2L_3+L_3L_1)+2(L_1^2L_2+L_2^2L_3+L_3^2L_1)+3L_1L_2L_3 \tag{6-68}$$

It can be verified that all the nine generalized displacements (3 nodal deflections, average deflections and average normal slopes along three sides) corresponding to w_α vanish.

The deflection field (6-66) is a complete cubic polynomial with 10 DOFs. When the internal DOF α is eliminated by a condensation process, only 9 external DOFs in $\boldsymbol{q}^e$ are retained.

From the deflection expression (6-66), the element curvature field $\boldsymbol{\kappa}$ can be expressed as

$$\boldsymbol{\kappa} = \boldsymbol{B}_q \boldsymbol{q}^e + \boldsymbol{B}_\alpha \alpha \tag{6-69}$$

The element stiffness matrix after condensation is

$$\boldsymbol{K}^e = \boldsymbol{K}_{qq} - \boldsymbol{K}_{\alpha q}{}^{\mathrm{T}} k_{\alpha\alpha}^{-1} \boldsymbol{K}_{\alpha q} \tag{6-70}$$

with

$$\boldsymbol{K}_{qq} = \iint_{A^e} \boldsymbol{B}_q{}^{\mathrm{T}} \boldsymbol{D} \boldsymbol{B}_q \mathrm{d}A$$

$$\boldsymbol{K}_{\alpha q} = \iint_{A^e} \boldsymbol{B}_\alpha{}^{\mathrm{T}} \boldsymbol{D} \boldsymbol{B}_q \mathrm{d}A$$

$$k_{\alpha\alpha} = \iint_{A^e} \boldsymbol{B}_\alpha{}^{\mathrm{T}} \boldsymbol{D} \boldsymbol{B}_\alpha \mathrm{d}A$$

$\boldsymbol{D}$ is the elastic matrix.

Example 6.6 The central deflection w_C (in Table 6.7) and central moment M_C (in Table 6.8) of a simply-supported square plate subjected to uniform load q. The length of the square plate side is L; the Poisson's ratio is 0.3. Two mesh orientations A and B (see Fig. 6.2) are considered. And, the numbers in parentheses are relative errors.

Table 6.7 The central deflection of a simply-supported square plate

Mesh 1/4 plate	LZ1		LZ2		CT		E-1	
	Mesh A	Mesh B	Mesh A	Mesh B	Mesh A	Mesh B	Mesh A	Mesh B
2×2	0.3817 (−6.0%)	0.3947 (−2.8%)	0.4005 (−1.4%)	0.4023 (−1.0%)	0.399 30 (−1.7%)	0.351 18 (−13.6%)	0.399 19 (−1.7%)	0.356 20 (−12.3%)
4×4	0.4009 (−1.3%)	0.4038 (−0.6%)	0.4047 (−0.4%)	0.4058 (−0.1%)	0.404 39 (−0.5%)	0.392 80 (−3.3%)	0.404 71 (−0.4%)	0.394 17 (−3.0%)
6×6	0.4040 (−0.6%)	0.4053 (−0.2%)	0.4056 (−0.2%)	0.4061 (0.0%)	0.405 40 (−0.2%)	0.400 28 (−1.5%)	0.405 61 (−0.2%)	0.400 92 (−1.3%)
8×8	0.4050 (−0.3%)	0.4057 (−0.1%)	0.4059 (−0.1%)	0.4062 (0.0%)				
Analytical	0.406 235$qL^4/(100D)$							

Table 6.8 The central moment of a simply-supported square plate

Mesh 1/4 plate	LZ1		LZ2		CT		E-1	
	Mesh *A*	Mesh *B*	Mesh *A*	Mesh *B*	Mesh *A*	Mesh *B*	Mesh *A*	Mesh *B*
2×2	0.4931 (3.0%)	0.5004 (4.5%)	0.5046 (5.4%)	0.5151 (7.6%)	0.499 88 (4.4%)	0.439 58 (−8.2%)	0.513 01 (7.1%)	0.468 71 (−2.1%)
4×4	0.4873 (1.8%)	0.4874 (1.8%)	0.4792 (0.1%)	0.4919 (2.7%)	0.483 47 (1.0%)	0.470 05 (−1.8%)	0.487 31 (1.8%)	0.477 97 (−0.2%)
6×6	0.4762 (−0.6%)	0.4839 (1.0%)	0.4778 (−0.2%)	0.4857 (1.4%)	0.480 90 (0.4%)	0.474 93 (−0.8%)	0.482 44 (0.7%)	0.478 71 (0.0%)
8×8	0.4768 (−0.4%)	0.4822 (0.7%)	0.4777 (−0.2%)	0.4832 (0.9%)				
Analytical	$0.478\,86qL^2/10$							

Since the elements CT[11], E-1 and E-2[12] have ever been identified as the most accurate nine-DOF triangular thin plate elements, the accuracy of the present two elements LZ1 and LZ2 is compared with those models.

From Tables 6.7 and 6.8, it can be seen that both elements LZ1 and LZ2 have high precision, their accuracy is at the same level as that of the elements CT and E-1.

6.3.3 Triangular Element GPL-T9[13]

The element nodal displacement vector $\boldsymbol{q}^e$ is the same as that of the elements LZ1 and LZ2. The element deflection field w is still assumed to be an incomplete cubic polynomial with nine unknown coefficients, i.e., Eq. (6-51). But, the nine basis functions are different and selected as follows

$$\boldsymbol{F}_\lambda = [L_1 \quad L_2 \quad L_3 \quad L_1L_2 \quad L_2L_3 \quad L_3L_1 \quad F_7 \quad F_8 \quad F_9] \tag{6-71}$$

where

$$\left.\begin{aligned} F_7 &= L_1\left(L_1-\frac{1}{2}\right)(L_1-1) \\ F_8 &= L_2\left(L_2-\frac{1}{2}\right)(L_2-1) \\ F_9 &= L_3\left(L_3-\frac{1}{2}\right)(L_3-1) \end{aligned}\right\} \tag{6-72}$$

In order to solve the nine unknown coefficients in $\boldsymbol{\lambda}$, we still select 9 conforming conditions according to the line-point conforming combination scheme, as shown in Eqs. (6-53) and (6-54).

Firstly, from the point condition (6-53), we obtain

$$\lambda_1 = w_1, \quad \lambda_2 = w_2, \quad \lambda_3 = w_3 \tag{6-73}$$

Secondly, from the first three average line conforming conditions about w in Eq. (6-54), λ_4, λ_5 and λ_6 can be obtained as

$$\left.\begin{aligned}
\lambda_4 &= \frac{c_3}{2}(\psi_{x1}-\psi_{x2})-\frac{b_3}{2}(\psi_{y1}-\psi_{y2})\\
\lambda_5 &= \frac{c_1}{2}(\psi_{x2}-\psi_{x3})-\frac{b_1}{2}(\psi_{y2}-\psi_{y3})\\
\lambda_6 &= \frac{c_2}{2}(\psi_{x3}-\psi_{x1})-\frac{b_2}{2}(\psi_{y3}-\psi_{y1})
\end{aligned}\right\} \tag{6-74}$$

Finally, from the last three average line conforming conditions about ψ_n in Eq. (6-54), λ_7, λ_8 and λ_9 can be obtained as

$$\left.\begin{aligned}
\lambda_7 &= -2w_1+(1+r_1)w_2+(1-r_1)w_3+\frac{1}{2}(c_2-c_3)\psi_{x1}+\frac{1}{2}(r_1c_1-c_3)\psi_{x2}\\
&\quad+\frac{1}{2}(r_1c_1+c_2)\psi_{x3}-\frac{1}{2}(b_2-b_3)\psi_{y1}-\frac{1}{2}(r_1b_1-b_3)\psi_{y2}-\frac{1}{2}(r_1b_1+b_2)\psi_{y3}\\
\lambda_8 &= (1-r_2)w_1-2w_2+(1+r_2)w_3+\frac{1}{2}(r_2c_2+c_3)\psi_{x1}+\frac{1}{2}(c_3-c_1)\psi_{x2}\\
&\quad+\frac{1}{2}(r_2c_2-c_1)\psi_{x3}-\frac{1}{2}(r_2b_2+b_3)\psi_{y1}-\frac{1}{2}(b_3-b_1)\psi_{y2}-\frac{1}{2}(r_2b_2-b_1)\psi_{y3}\\
\lambda_9 &= (1+r_3)w_1+(1-r_3)w_2-2w_3+\frac{1}{2}(r_3c_3-c_2)\psi_{x1}+\frac{1}{2}(r_3c_3+c_1)\psi_{x2}\\
&\quad+\frac{1}{2}(c_1-c_2)\psi_{x3}-\frac{1}{2}(r_3b_3-b_2)\psi_{y1}-\frac{1}{2}(r_3b_3+b_1)\psi_{y2}-\frac{1}{2}(b_1-b_2)\psi_{y3}
\end{aligned}\right\} \tag{6-75}$$

After $\boldsymbol{\lambda}$ is solved, the deflection field w can be expressed in terms of the shape functions

$$w=\sum_{i=1}^{3}(N_i w_i+N_{xi}\psi_{xi}+N_{yi}\psi_{yi}) \tag{6-76}$$

where

$$\left.\begin{aligned}
N_1 &= L_1-2F_7+(1-r_2)F_8+(1+r_3)F_9\\
N_{x1} &= \frac{c_3}{2}L_1L_2-\frac{c_2}{2}L_3L_1+\frac{1}{2}(c_2-c_3)F_7+\frac{1}{2}(r_2c_2+c_3)F_8+\frac{1}{2}(r_3c_3-c_2)F_9\\
N_{y1} &= -\frac{b_3}{2}L_1L_2+\frac{b_2}{2}L_3L_1-\frac{1}{2}(b_2-b_3)F_7-\frac{1}{2}(r_2b_2+b_3)F_8-\frac{1}{2}(r_3b_3-b_2)F_9
\end{aligned}\right\} \tag{6-77}$$

The expressions for the other six shape functions can be obtained by permutation.

And, b_i, c_i and r_i are given by Eq. (6-58). Based on these shape functions, the element stiffness matrix can be derived by the conventional procedure.

Example 6.7 The central deflection and central moment for the simply-supported and clamped square plates subjected to uniform load q and central concentrated load P. The meshes A and B in Fig. 6.2, and mesh C in Fig. 6.13 are used. Results by the element GPL-T9 are listed in Tables 6.9 to 6.11.

Example 6.8 The central deflection of a simply-supported circular plate subjected to uniform load.

Due to symmetry, only one quarter of the plate is modelled. Two meshes shown in Fig. 6.14 are used. The computational errors of the central deflection obtained by the element GPL-T9 are given in Table 6.12. And, the results of reference [14] are also listed for comparison.

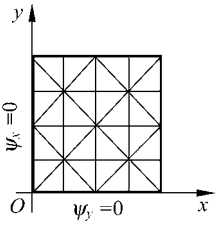

Figure 6.13 Mesh C 4×4 for a quarter square plate

Table 6.9 The central deflection of simply-supported and clamped square plates subjected to uniform load q

Mesh (1/4 plate)	Clamped			Simply-supported		
	Mesh A	Mesh B	Mesh C	Mesh A	Mesh B	Mesh C
2×2	0.1170	0.0995	0.0985	0.3804	0.3948	0.3829
4×4	0.1241	0.1192	0.1210	0.4007	0.4038	0.4008
6×6	0.1256	0.1233	0.1240	0.4040	0.4054	0.4039
8×8	0.1261	0.1246	0.1251	0.4046	0.4049	0.4044
Analytical	$0.126\,53qL^4/(100D)$			$0.406\,24qL^4/(100D)$		

Table 6.10 The central moment of simply-supported and clamped square plates subjected to uniform load q

Mesh (1/4 plate)	Clamped			Simply-supported		
	Mesh A	Mesh B	Mesh C	Mesh A	Mesh B	Mesh C
2×2	0.3054	0.2185	0.2216	0.4958	0.4986	0.5296
4×4	0.2395	0.2274	0.2405	0.4775	0.4869	0.4967
6×6	0.2329	0.2286	0.2342	0.4770	0.4838	0.4871
8×8	0.2309	0.2288	0.2319	0.4777	0.4811	0.4829
Analytical	$0.2291qL^2/10$			$0.4789qL^2/10$		

Table 6.11 The central deflection of simply-supported and clamped square plates subjected to central concentrated load P

Mesh (1/4 plate)	Clamped			Simply-supported		
	Mesh A	Mesh B	Mesh C	Mesh A	Mesh B	Mesh C
2×2	0.4655	0.4466	0.4235	1.0183	1.0912	1.0501
4×4	0.5311	0.5269	0.5257	1.1211	1.1382	1.1253
6×6	0.5470	0.5448	0.5434	1.1422	1.1498	1.1430
8×8	0.5527	0.5513	0.5503	1.1484	1.1518	1.1485
Analytical	$0.5612PL^2/(100D)$			$1.160PL^2/(100D)$		

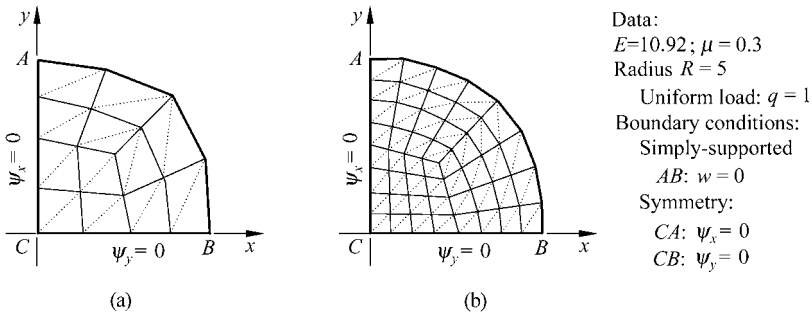

Figure 6.14 The typical mesh for 1/4 circular plate

(a) 24 triangular elements or 12 quadrilateral elements; (b) 96 triangular elements or 48 quadrilateral elements

Table 6.12 The computational errors of the central deflection of a simply-supported circular plate subjected to uniform load

Mesh (1/4 plate)	GPL-T9	Reference [14]
Mesh A	0.63%	2.87%
Mesh B	0.10%	0.70%

Example 6.9 The central deflection w and central moment M_y of a rhombus plate (Fig. 6.15) subjected to uniform load (Razzaque's skew plate problem).

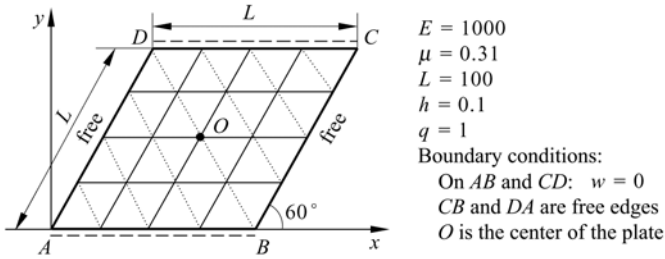

Figure 6.15 Razzaque's skew plate: typical mesh 4×4

The mesh used is shown in Fig. 6.15 and the results by the element GPL-T9 and other models are listed in Table 6.13. It can be seen that the performance of the element GPL-T9 is better than those of the other elements in references [15] and [16].

Table 6.13 The central deflection and central moment of a rhombus plate subjected to uniform load

DOFs	Mesh	Central deflection w			Central moment M_y		
		GPL-T9	Reference [15]	Reference [16]	GPL-T9	Reference [15]	Reference [16]
27	2×2	0.7318	0.7230		1.0140	0.7602	
75	4×4	0.7783	0.7718	0.8414	0.9925	0.9172	0.9761
105	4×6	0.7941	0.7850		0.9904	0.9473	
243	8×8	0.7890		0.8111	0.9565		0.9739
507	12×12	0.7913		0.8057	0.9596		0.9688
Difference method[15]		$0.7945qL^4/(100D)$			$0.9589qL^2/10$		

6.4 Super-Basis Line-Point Conforming Scheme—Elements GCⅢ-R12 and GCⅢ-T9

This section will introduce the construction procedure for the super-basis thin plate elements formulated by the combination scheme of the line conforming and point conforming conditions. The no. 12, 13, 14 and 15 elements GCⅢ-R12, GPL-R1, GCⅢ-T9 and LZ3 in Table 5.1 all belong to this element group. Two elements GCⅢ-R12 and GCⅢ-T9 will be discussed in detail.

6.4.1 Rectangular Element GCⅢ-R12—Improvement on the Element ACM

The rectangular thin plate element GCⅢ-R12 is a model developed by improving the element ACM[6]. Element ACM employed a conventional scheme: let $m=n=12$, the 12 conforming conditions are all point conforming conditions. Though the deflection along the element boundary is compatible, the normal slope along the element boundary is incompatible, and does not satisfy the average line conforming conditions. Therefore, an improvement scheme is proposed: let $m>n=12$, then, besides the 12 point conforming conditions, the average line conforming conditions of the normal slope along the element sides are supplemented. Thereupon, the element compatibility is improved, and the new element GCⅢ-R12 is obtained.

The detailed construction procedure for the element GCⅢ-R12 is as follows.

Assume that the element deflection field w consists of two parts

$$w = \overline{w}(\mathrm{ACM}) + \hat{w} \tag{6-78}$$

where $\overline{w}$ (ACM) is the interpolation formula with 12 unknown coefficients used by the element ACM

$$\begin{aligned}\overline{w} = {} & \lambda_1 + \lambda_2\xi + \lambda_3\eta + \lambda_4\xi^2 + \lambda_5\xi\eta + \lambda_6\eta^2 + \lambda_7\xi^3 \\ & + \lambda_8\xi^2\eta + \lambda_9\xi\eta^2 + \lambda_{10}\eta^3 + \lambda_{11}\xi^3\eta + \lambda_{12}\xi\eta^3\end{aligned} \tag{6-79}$$

$\hat{w}$ is the additional deflection field with two new unknown coefficients

$$\hat{w} = \lambda_{13}\xi(\xi^2-1)(\eta^2-1) + \lambda_{14}\eta(\xi^2-1)(\eta^2-1) \tag{6-80}$$

$\hat{w}$ possesses the following characteristics:

(1) At the four corner nodes, $\hat{w}$, $\dfrac{\partial\hat{w}}{\partial x}$ and $\dfrac{\partial\hat{w}}{\partial y}$ are all zero;

(2) Along four element boundary lines, $\hat{w}$ identically equals to zero (thus $\dfrac{\partial\hat{w}}{\partial s}$ also identically equals to zero), but $\dfrac{\partial\hat{w}}{\partial n}$ does not identically equal to zero.

The deflection field expressed by Eq. (6-78) is an incomplete bi-cubic polynomial with 14 unknown coefficients. Owing to $m > n$, this is a super-basis element.

In order to solve 14 unknown coefficients, 14 conforming conditions are needed.

Firstly, the 12 point conforming conditions about w, ψ_x and ψ_y at the 4 corner nodes are applied. Due to the characteristic (1) of the additional deflection $\hat{w}$, we know that λ_{13} and λ_{14} will not appear in these 12 point conforming conditions. So, the 12 unknown coefficients $\lambda_1, \lambda_2, \cdots, \lambda_{12}$ can just be solved by the 12 conditions. That is to say, the solutions of these unknown coefficients are identical with those of the element ACM.

Secondly, we apply the average line conforming conditions about normal slopes:

$$\left.\begin{aligned}\int_{-1}^{1}\left(\frac{\partial w}{\partial x}\right)_{23}\mathrm{d}\eta &= \int_{-1}^{1}\tilde{\psi}_{x23}\mathrm{d}\eta \\ \int_{-1}^{1}\left(\frac{\partial w}{\partial x}\right)_{14}\mathrm{d}\eta &= \int_{-1}^{1}\tilde{\psi}_{x14}\mathrm{d}\eta \\ \int_{-1}^{1}\left(\frac{\partial w}{\partial y}\right)_{43}\mathrm{d}\xi &= \int_{-1}^{1}\tilde{\psi}_{y43}\mathrm{d}\xi \\ \int_{-1}^{1}\left(\frac{\partial w}{\partial y}\right)_{12}\mathrm{d}\xi &= \int_{-1}^{1}\tilde{\psi}_{y12}\mathrm{d}\xi\end{aligned}\right\} \tag{6-81}$$

In Eq. (6-81), there seemingly are four conditions, in which only two conditions

are independent. Then λ_{13} and λ_{14} can be derived as follows:

$$\left.\begin{aligned}\lambda_{13} &= -\frac{b}{16}\sum_{i=1}^{4}\psi_{yi}\xi_i\eta_i \\ \lambda_{14} &= -\frac{a}{16}\sum_{i=1}^{4}\psi_{xi}\xi_i\eta_i\end{aligned}\right\} \tag{6-82}$$

After the determination of the 14 unknown coefficients, the element deflection field and its shape functions can be obtained:

$$w=\sum_{i=1}^{4}(N_i w_i + N_{xi}\psi_{xi} + N_{yi}\psi_{yi}) \tag{6-83}$$

where the shape functions are all constituted of two parts:

$$\left.\begin{aligned}N_i &= \bar{N}_i + \hat{N}_i \\ N_{xi} &= \bar{N}_{xi} + \hat{N}_{xi} \\ N_{yi} &= \bar{N}_{yi} + \hat{N}_{yi}\end{aligned}\right\} \quad (i=1,2,3,4) \tag{6-84}$$

$\bar{N}_i$, $\bar{N}_{xi}$ and $\bar{N}_{yi}$ belong to the part related to $\bar{w}$ (refer to Eq. (7-19)); $\hat{N}_i$, $\hat{N}_{xi}$ and $\hat{N}_{yi}$ belong to the part related to $\hat{w}$:

$$\left.\begin{aligned}\hat{N}_i &= 0 \\ \hat{N}_{xi} &= -\frac{a}{16}\xi_i\eta_i\eta(1-\eta^2)(1-\xi^2) \\ \hat{N}_{yi} &= -\frac{b}{16}\xi_i\eta_i\xi(1-\xi^2)(1-\eta^2)\end{aligned}\right\} \quad (i=1,2,3,4) \tag{6-85}$$

Since the shape functions have been obtained, the element stiffness matrix can then be established.

Note that, actually, only one of the first two conditions in Eq. (6-81) is independent, this is because of the following relation

$$\int_{-1}^{1}\left[\left(\frac{\partial w}{\partial x}\right)_{23}-\left(\frac{\partial w}{\partial x}\right)_{14}\right]\mathrm{d}\eta=\int_{-1}^{1}(\tilde{\psi}_{x23}-\tilde{\psi}_{x14})\mathrm{d}\eta \tag{6-86}$$

Here, the proof of Eq. (6-86) is given as follows.

Firstly, from Eq. (6-80), we obtain

$$\int_{-1}^{1}\left[\left(\frac{\partial \hat{w}}{\partial x}\right)_{23}-\left(\frac{\partial \hat{w}}{\partial x}\right)_{14}\right]\mathrm{d}\eta=0 \tag{6-87}$$

Secondly, it can be verified that the deflection field $\bar{w}$ of the element ACM

satisfies the perimeter conforming condition under constant internal force state (refer to Sect. 7.2). Now, consider the following constant internal force state:

$$M_x = \beta_1, \quad M_y = 0, \quad M_{xy} = 0$$

Then, the boundary forces of the rectangular element can be obtained from Eq. (5-8):

$$\begin{aligned} &Q_n = 0, \qquad M_{ns} = 0 \\ &(M_n)_{12} = (M_n)_{34} = 0 \\ &(M_n)_{23} = (M_n)_{14} = \beta_1 \end{aligned}$$

Substitution of the above equation into the perimeter conforming condition (5-2a) yields

$$\int_{-1}^{1} \left[\left(\frac{\partial \overline{w}}{\partial n} - \tilde{\psi}_n \right)_{23} + \left(\frac{\partial \overline{w}}{\partial n} - \tilde{\psi}_n \right)_{14} \right] \mathrm{d}\eta = 0$$

i.e.,

$$\int_{-1}^{1} \left[\left(\frac{\partial \overline{w}}{\partial x} - \tilde{\psi}_x \right)_{23} - \left(\frac{\partial \overline{w}}{\partial x} - \tilde{\psi}_x \right)_{14} \right] \mathrm{d}\eta = 0 \tag{6-88}$$

Since $w = \overline{w} + \hat{w}$, by the superposition of Eqs. (6-88) and (6-87), Eq. (6-86) can be obtained.

The above procedure proves that there is only one independent condition existing in the first two conditions of Eq. (6-81). Similarly, it can be verified that there is also only one independent condition existing in the last two conditions of Eq. (6-81).

Example 6.10 The central deflection w_C and central moment M_C of the simply-supported and clamped square plates subjected to uniform load q and central concentrated load P.

For comparison, results by the elements GCⅢ-R12 and ACM are given in Tables 6.14 and 6.15. The length of the square plate side is L, the Poisson's ratio is 0.3.

Table 6.14 The central deflection and moment of square plates subjected to uniform load q

Mesh (1/4 plate)	Central deflection w_C				Central moment M_C			
	Simply-supported		Clamped		Simply-supported		Clamped	
	ACM	GCⅢ-R12	ACM	GCⅢ-R12	ACM	GCⅢ-R12	ACM	GCⅢ-R12
2×2	0.433	0.395	0.140	0.120	0.522	0.434	0.278	0.203
4×4	0.413	0.403	0.133	0.123	0.489	0.466	0.241	0.221
6×6	0.409	0.405	0.128	0.126	0.483	0.473	0.234	0.225
8×8	0.408	0.406	0.128	0.126	0.482	0.476	0.232	0.227
Analytical	0.406 24$qL^4/(100D)$		0.126 53$qL^4/(100D)$		0.478 86$qL^2/10$		0.2291$qL^2/10$	

Table 6.15 The central deflection of square plates subjected to central concentrated load P

Mesh (1/4 plate)	Simply-supported		Clamped	
	ACM	GCⅢ-R12	ACM	GCⅢ-R12
2×2	0.123	0.111	0.613	0.523
4×4	0.118	0.115	0.580	0.549
6×6	0.117	0.115	0.571	0.555
8×8	0.117	0.116	0.567	0.558
Analytical	$0.1160PL^2/(10D)$		$0.5612PL^2/(100D)$	

From Tables 6.14 and 6.15, it can be seen that the accuracy of the element GC Ⅲ-R12 is better than that of the element ACM.

6.4.2 Triangular Element GCⅢ-T9

The construction procedure for the element GCⅢ-T9 is: the assumed element deflection field contains 12 unknown coefficients ($m=12$, $n=9$, it is a super-basis element); the 12 conforming conditions used include 9 point conforming conditions and 3 average line conforming conditions. Following is the detailed derivation procedure of the element.

The element deflection field is assumed as

$$\begin{aligned} w = {} & \lambda_1 L_1 + \lambda_2 L_2 + \lambda_3 L_3 + \lambda_4 L_2 L_3 + \lambda_5 L_3 L_1 + \lambda_6 L_1 L_2 \\ & + \lambda_7 (L_3 - L_2) L_2 L_3 + \lambda_8 (L_1 - L_3) L_3 L_1 + \lambda_9 (L_2 - L_1) L_1 L_2 \\ & + \lambda_{10} L_1 L_2 L_3^2 + \lambda_{11} L_2 L_3 L_1^2 + \lambda_{12} L_3 L_1 L_2^2 \end{aligned} \tag{6-89}$$

The element rotation fields are as follows:

$$\left.\begin{aligned} \psi_x &= \frac{\partial w}{\partial x} = \frac{1}{2A}\left(b_1 \frac{\partial w}{\partial L_1} + b_2 \frac{\partial w}{\partial L_2} + b_3 \frac{\partial w}{\partial L_3} \right) \\ \psi_y &= \frac{\partial w}{\partial y} = \frac{1}{2A}\left(c_1 \frac{\partial w}{\partial L_1} + c_2 \frac{\partial w}{\partial L_2} + c_3 \frac{\partial w}{\partial L_3} \right) \end{aligned}\right\} \tag{6-90}$$

In order to solve 12 unknown coefficients, 12 conforming conditions are needed. Firstly, 9 point conforming conditions at the corner nodes are selected as

$$\left.\begin{aligned}
&w_1 = \lambda_1 \\
&\psi_{x1} = \frac{1}{2A}[b_1\lambda_1 + b_2(\lambda_2 + \lambda_6 - \lambda_9) + b_3(\lambda_3 + \lambda_5 + \lambda_8)] \\
&\psi_{y1} = \frac{1}{2A}[c_1\lambda_1 + c_2(\lambda_2 + \lambda_6 - \lambda_9) + c_3(\lambda_3 + \lambda_5 + \lambda_8)] \\
&w_2 = \lambda_2 \\
&\psi_{x2} = \frac{1}{2A}[b_1(\lambda_1 + \lambda_6 + \lambda_9) + b_2\lambda_2 + b_3(\lambda_3 + \lambda_4 - \lambda_7)] \\
&\psi_{y2} = \frac{1}{2A}[c_1(\lambda_1 + \lambda_6 + \lambda_9) + c_2\lambda_2 + c_3(\lambda_3 + \lambda_4 - \lambda_7)] \\
&w_3 = \lambda_3 \\
&\psi_{x3} = \frac{1}{2A}[b_1(\lambda_1 + \lambda_5 - \lambda_8) + b_2(\lambda_2 + \lambda_4 + \lambda_7) + b_3\lambda_3] \\
&\psi_{y3} = \frac{1}{2A}[c_1(\lambda_1 + \lambda_5 - \lambda_8) + c_2(\lambda_2 + \lambda_4 + \lambda_7) + c_3\lambda_3]
\end{aligned}\right\} \tag{6-91}$$

These 9 conditions do not contain λ_{10}, λ_{11} and λ_{12}, so the first 9 unknown coefficients can be solved as follows:

$$\left.\begin{aligned}
&\lambda_1 = w_1 \\
&\lambda_2 = w_2 \\
&\lambda_3 = w_3 \\
&\lambda_4 = \frac{c_1}{2}(\psi_{x2} - \psi_{x3}) - \frac{b_1}{2}(\psi_{y2} - \psi_{y3}) \\
&\lambda_5 = \frac{c_2}{2}(\psi_{x3} - \psi_{x1}) - \frac{b_2}{2}(\psi_{y3} - \psi_{y1}) \\
&\lambda_6 = \frac{c_3}{2}(\psi_{x1} - \psi_{x2}) - \frac{b_3}{2}(\psi_{y1} - \psi_{y2}) \\
&\lambda_7 = -w_2 + w_3 - \frac{c_1}{2}(\psi_{x2} + \psi_{x3}) - \frac{b_1}{2}(\psi_{y2} + \psi_{y3}) \\
&\lambda_8 = -w_3 + w_1 - \frac{c_2}{2}(\psi_{x3} + \psi_{x1}) - \frac{b_2}{2}(\psi_{y3} + \psi_{y1}) \\
&\lambda_9 = -w_1 + w_2 - \frac{c_3}{2}(\psi_{x1} + \psi_{x2}) - \frac{b_3}{2}(\psi_{y1} + \psi_{y2})
\end{aligned}\right\} \tag{6-92}$$

From Eq. (6-89), it can be seen that the deflection along each element side is a cubic polynomial (note: three terms corresponding to λ_{10}, λ_{11}, λ_{12} are all zero along the boundary line), and can be determined uniquely according to the values of deflections and tangential rotations at the two ends of the side. Thereby, when

the 9 point conforming conditions at the corner nodes are satisfied, the deflection along each element side is compatible exactly. But, the normal slope $\psi_n = \dfrac{\partial w}{\partial n}$ along each element side is still incompatible.

Secondly, in order to require the normal slope along each side to satisfy the necessary conforming conditions, 3 average line conforming conditions are imposed on the normal slopes along the element sides:

$$\int_0^{d_3}\left(\frac{\partial w}{\partial n}-\tilde{\psi}_n\right)\Big|_{L_3=0}\mathrm{d}s=0 \tag{6-93a}$$

$$\int_0^{d_1}\left(\frac{\partial w}{\partial n}-\tilde{\psi}_n\right)\Big|_{L_1=0}\mathrm{d}s=0 \tag{6-93b}$$

$$\int_0^{d_2}\left(\frac{\partial w}{\partial n}-\tilde{\psi}_n\right)\Big|_{L_2=0}\mathrm{d}s=0 \tag{6-93c}$$

where d_1, d_2 and d_3 denote the length of each element side, respectively (Fig. 6.1). Substitution of Eq. (6-90) into the above equation will yield three equations containing λ_{10}, λ_{11}, λ_{12}. Now, we take Eq. (6-93a) as an example, the derivation procedure is listed as follows:

The normal derivative of the deflection field (6-89) along side $\overline{12}$ ($L_3=0$) is:

$$\begin{aligned}\left.\frac{\partial w}{\partial n}\right|_{L_3=0} &= \frac{d_3}{4A}\left[(1+r_3)\frac{\partial w}{\partial L_1}+(1-r_3)\frac{\partial w}{\partial L_2}-2\frac{\partial w}{\partial L_3}\right]_{L_3=0}\\ &= \frac{d_3}{4A}\{(1+r_3)[\lambda_1+\lambda_6L_2+\lambda_9L_2(L_2-2L_1)]+(1-r_3)[\lambda_2+\lambda_6L_1+\lambda_9L_1(2L_2-L_1)]\\ &\quad -2[\lambda_3+\lambda_4L_2+\lambda_5L_1-\lambda_7L_2^2+\lambda_8L_1^2+\lambda_{11}L_2L_1^2+\lambda_{12}L_1L_2^2]\}\end{aligned} \tag{6-94}$$

where

$$r_3=\frac{d_1^2-d_2^2}{d_3^2},\quad r_1=\frac{d_2^2-d_3^2}{d_1^2},\quad r_2=\frac{d_3^2-d_1^2}{d_2^2} \tag{6-95}$$

The integration of Eq. (6-94) along side $\overline{12}$ is

$$\int_0^{d_3}\left.\frac{\partial w}{\partial n}\right|_{L_3=0}\mathrm{d}s=\frac{d_3^2}{4A}\left[(1+r_3)\lambda_1+(1-r_3)\lambda_2-2\lambda_3-\lambda_4-\lambda_5+\lambda_6+\frac{2}{3}\lambda_7-\frac{2}{3}\lambda_8-\frac{\lambda_{11}}{6}-\frac{\lambda_{12}}{6}\right] \tag{6-96}$$

And, the integration of the normal slope $\tilde{\psi}_n$ along side $\overline{12}$ is

$$\int_0^{d_3}\tilde{\psi}_n\big|_{L_3=0}\mathrm{d}s=-\frac{b_3}{2}(\psi_{x1}+\psi_{x2})-\frac{c_3}{2}(\psi_{y1}+\psi_{y2}) \tag{6-97}$$

Substitution of Eq. (6-91) into the above equation yields

$$\int_0^{d_3} \tilde{\psi}_n\big|_{L_3=0} \mathrm{d}s = \frac{d_3^2}{4A}[(1+r_3)\lambda_1 + (1-r_3)\lambda_2 - 2\lambda_3 - \lambda_4 - \lambda_5 + \lambda_6 + \lambda_7 - \lambda_8 + r_3\lambda_9] \tag{6-98}$$

Substitution of Eqs. (6-96) and (6-98) into Eq. (6-93a) yields the first equation of (6-99)

$$\left.\begin{aligned} \lambda_{11} + \lambda_{12} &= -2\lambda_7 + 2\lambda_8 - 6r_3\lambda_9 \\ \lambda_{12} + \lambda_{10} &= -2\lambda_8 + 2\lambda_9 - 6r_1\lambda_7 \\ \lambda_{10} + \lambda_{11} &= -2\lambda_9 + 2\lambda_7 - 6r_2\lambda_8 \end{aligned}\right\} \tag{6-99}$$

Similarly, the second and third equations in the above equations can also be derived. Then, λ_{10}, λ_{11} and λ_{12} can be solved from Eq. (6-99):

$$\left.\begin{aligned} \lambda_{10} &= (2-3r_1)\lambda_7 - (2+3r_2)\lambda_8 + 3r_3\lambda_9 \\ \lambda_{11} &= 3r_1\lambda_7 + (2-3r_2)\lambda_8 - (2+3r_3)\lambda_9 \\ \lambda_{12} &= -(2+3r_1)\lambda_7 + 3r_2\lambda_8 + (2-3r_3)\lambda_9 \end{aligned}\right\} \tag{6-100}$$

Now, all the 12 unknown coefficients have been obtained, as shown in Eqs. (6-92) and (6-100). Substituting them into Eq. (6-89), the element deflection field and its shape functions can be derived as follows:

$$w = \sum_{i=1}^{3} (N_i w_i + N_{xi}\psi_{xi} + N_{yi}\psi_{yi}) \tag{6-101}$$

The three shape functions of the node 1 are

$$\left.\begin{aligned} N_1 &= L_1 + L_1L_3(L_1 - L_3) - L_1L_2(L_2 - L_1) - (2 + 3r_2 + 3r_3)L_1L_2L_3^2 \\ &\quad + (4 - 3r_2 + 3r_3)L_2L_3L_1^2 - (2 - 3r_2 - 3r_3)L_3L_1L_2^2 \\ N_{x1} &= -\frac{c_2}{2}L_3L_1 + \frac{c_3}{2}L_1L_2 - \frac{c_2}{2}(L_1 - L_3)L_3L_1 - \frac{c_3}{2}(L_2 - L_1)L_1L_2 + \frac{1}{2}(2c_2 + 3c_2r_2 \\ &\quad - 3c_3r_3)L_1L_2L_3^2 - \frac{1}{2}(2c_2 - 2c_3 - 3c_2r_2 - 3c_3r_3)L_2L_3L_1^2 \\ &\quad - \frac{1}{2}(2c_3 + 3c_2r_2 - 3c_3r_3)L_3L_1L_2^2 \\ N_{y1} &= \frac{b_2}{2}L_3L_1 - \frac{b_3}{2}L_1L_2 + \frac{b_2}{2}(L_1 - L_3)L_3L_1 + \frac{b_3}{2}(L_2 - L_1)L_1L_2 \\ &\quad - \frac{1}{2}(2b_2 + 3b_2r_2 - 3b_3r_3)L_1L_2L_3^2 + \frac{1}{2}(2b_2 - 2b_3 - 3b_2r_2 - 3b_3r_3)L_2L_3L_1^2 \\ &\quad + \frac{1}{2}(2b_3 + 3b_2r_2 - 3b_3r_3)L_3L_1L_2^2 \end{aligned}\right\} \tag{6-102}$$

The shape functions of the nodes 2 and 3 can be obtained by permutation. By these shape functions, it is easy to derive the element stiffness matrix, which has been given in reference [17].

Note that Eq. (6-99) can also be derived from the point conforming conditions about ψ_n at the mid-points of the element sides. This can be explained as follows: according to the deflection field assumed in Eq. (6-89), the normal slope $\psi_n = \dfrac{\partial w}{\partial n}$ along each side is cubically distributed. On conditions that ψ_n is cubically distributed along the element side and has already satisfied the point conforming conditions at the two ends, the average line conforming condition of ψ_n is equivalent to the point conforming condition of ψ_n at mid-side point.

Example 6.11 The central deflection w_C and central moment M_C of the simply-supported and clamped square plates subjected to uniform load q and central concentrated load P.

The length of the square plate side is L, the Poisson's ratio is 0.3. Two mesh types are used: mesh B in Fig. 6.2 and Mesh C in Fig. 6.13. The results by the element GCⅢ-T9 are given in Tables 6.16 and 6.17.

Table 6.16 The central deflection and moment of square plates subjected to uniform load (GCⅢ-T9)

Mesh (1/4 plate)	Central deflection w_C				Central moment M_C			
	Simply-supported		Clamped		Simply-supported		Clamped	
	Mesh B	Mesh C	Mesh B	Mesh C	Mesh B	Mesh C	Mesh B	Mesh C
2×2	0.394	0.386	0.101	0.100	0.472	0.547	0.198	0.230
4×4	0.403	0.402	0.120	0.120	0.479	0.502	0.222	0.244
6×6	0.405	0.404	0.123	0.124	0.480	0.489	0.226	0.236
8×8	0.404	0.405	0.125	0.125	0.478	0.485	0.227	0.233
Analytical	0.406 24 $qL^4/(100D)$		0.126 53 $qL^4/(100D)$		0.478 86 $qL^2/10$		0.2291 $qL^2/10$	

Table 6.17 The central deflection of square plates subjected to central concentrated load (GCⅢ-T9)

Mesh (1/4 plate)	Simply-supported		Clamped	
	Mesh B	Mesh C	Mesh B	Mesh C
2×2	0.107	0.106	0.438	0.433
4×4	0.113	0.113	0.523	0.527
6×6	0.115	0.114	0.542	0.544
8×8	0.115	0.115	0.550	0.551
Analytical	0.1160 $PL^2/(10D)$		0.5612 $PL^2/(100D)$	

6.5 Super-Basis Point Conforming Scheme—Elements MB1-T9 and MB2-T9

This and the next sections will introduce two construction schemes for the super-basis thin plate elements formulated only by the point conforming conditions, which are also the improvement schemes for the conventional non-conforming elements. Firstly, according to the conventional method of non-conforming elements, the point conforming conditions about w, ψ_x, ψ_y at the corner nodes are selected. Here, the normal slope ψ_n along each side is generally still incompatible. Secondly, for overcoming this shortcoming, the point conforming conditions of ψ_n at the mid-side points are supplemented for improving the compatibility of ψ_n along each side. The no. 16, 17 and 18 elements in Table 5.1 belong to this element group, in which two triangular elements MB1-T9 and MB2-T9 will be introduced in detail[18].

6.5.1 Triangular Element MB1-T9

Triangular element MB1-T9 has 9 DOFs. Its assumed deflection field contains 12 unknown coefficients, and can be written as the sum of two parts:

$$w = \overline{w} + \hat{w} \tag{6-103}$$

where $\overline{w}$ and $\hat{w}$ contain 9 and 3 unknown coefficients, respectively.

$$\overline{w}=\lambda_1 L_1+\lambda_2 L_2+\lambda_3 L_3+\lambda_4 L_1 L_2+\lambda_5 L_2 L_3+\lambda_6 L_3 L_1+\lambda_7 L_1^2 L_2+\lambda_8 L_2^2 L_3+\lambda_9 L_3^2 L_1 \tag{6-104}$$

$$\hat{w} = \lambda_{10} L_2^2 L_3^2 + \lambda_{11} L_3^2 L_1^2 + \lambda_{12} L_1^2 L_2^2 \tag{6-105}$$

The selected 12 conforming conditions are also classified into two groups. The first group involves 9 point conforming conditions about w, ψ_x and ψ_y at three corner nodes. Since $\hat{w}$, $\dfrac{\partial \hat{w}}{\partial x}$ and $\dfrac{\partial \hat{w}}{\partial y}$ at the corner nodes are identically equal zero, only the first 9 unknown coefficients $\lambda_1, \lambda_2, \cdots, \lambda_9$ appear in these 9 equations. Their solutions are

$$\left.\begin{aligned}
\lambda_1 &= w_1 \\
\lambda_2 &= w_2 \\
\lambda_3 &= w_3 \\
\lambda_4 &= -w_1 + w_2 - c_3\psi_{x2} + b_3\psi_{y2} \\
\lambda_5 &= -w_2 + w_3 - c_1\psi_{x3} + b_1\psi_{y3} \\
\lambda_6 &= -w_3 + w_1 - c_2\psi_{x1} + b_2\psi_{y1} \\
\lambda_7 &= 2w_1 - 2w_2 + c_3(\psi_{x1} + \psi_{x2}) - b_3(\psi_{y1} + \psi_{y2}) \\
\lambda_8 &= 2w_2 - 2w_3 + c_1(\psi_{x2} + \psi_{x3}) - b_1(\psi_{y2} + \psi_{y3}) \\
\lambda_9 &= 2w_3 - 2w_1 + c_2(\psi_{x3} + \psi_{x1}) - b_2(\psi_{y3} + \psi_{y1})
\end{aligned}\right\} \tag{6-106}$$

In the assumed deflection field $\overline{w}$ of Eq. (6-104), deflection $\overline{w}$ along each side is a cubic polynomial, and normal slope $\dfrac{\partial \overline{w}}{\partial n}$ is a quadric polynomial. Thereby, along each boundary line, $\overline{w}$ and $\tilde{w}$ conform to each other, but $\dfrac{\partial \overline{w}}{\partial n}$ and $\tilde{\psi}_n$ are not compatible. In fact, the non-conforming values of the normal slopes at the mid-side points 4, 5 and 6 can be solved as follows:

$$\begin{Bmatrix} \dfrac{1}{d_1}\left(\dfrac{\partial \overline{w}}{\partial n}-\tilde{\psi}_n\right)_4 \\ \dfrac{1}{d_2}\left(\dfrac{\partial \overline{w}}{\partial n}-\tilde{\psi}_n\right)_5 \\ \dfrac{1}{d_3}\left(\dfrac{\partial \overline{w}}{\partial n}-\tilde{\psi}_n\right)_6 \end{Bmatrix} = \frac{1}{16A}\begin{bmatrix} 0 & 1+3r_1 & 2 \\ 2 & 0 & 1+3r_2 \\ 1+3r_3 & 2 & 0 \end{bmatrix}\begin{Bmatrix} \lambda_7 \\ \lambda_8 \\ \lambda_9 \end{Bmatrix} \tag{6-107}$$

where d_1 and point 4 are the length and mid-side point of the opposite side of the node 1, respectively; r_1 is given by Eq. (6-58). The rest can be analogized.

The second group involves the point conforming conditions about ψ_n at the mid-side points. Since

$$\begin{Bmatrix} \dfrac{1}{d_1}\left(\dfrac{\partial \hat{w}}{\partial n}\right)_4 \\ \dfrac{1}{d_2}\left(\dfrac{\partial \hat{w}}{\partial n}\right)_5 \\ \dfrac{1}{d_3}\left(\dfrac{\partial \hat{w}}{\partial n}\right)_6 \end{Bmatrix} = \frac{1}{8A}\begin{Bmatrix} \lambda_{10} \\ \lambda_{11} \\ \lambda_{12} \end{Bmatrix} \tag{6-108}$$

from Eqs. (6-107) and (6-108), and according to the conforming conditions of ψ_n, we obtain

$$\begin{Bmatrix} \lambda_{10} \\ \lambda_{11} \\ \lambda_{12} \end{Bmatrix} = -\frac{1}{2}\begin{bmatrix} 0 & 1+3r_1 & 2 \\ 2 & 0 & 1+3r_2 \\ 1+3r_3 & 2 & 0 \end{bmatrix}\begin{Bmatrix} \lambda_7 \\ \lambda_8 \\ \lambda_9 \end{Bmatrix} \tag{6-109}$$

Thus, all the unknown coefficients have been solved out, and the shape functions and element stiffness matrix can be obtained by the conventional procedure.

Here, we also give the following two points.

(1) If we substitute Eq. (6-109) into Eq. (6-105), then w in Eq. (6-103) can be written in terms of the first 9 unknown coefficients:

$$w = \lambda_1 L_1 + \lambda_2 L_2 + \lambda_3 L_3 + \lambda_4 L_1 L_2 + \lambda_5 L_2 L_3 + \lambda_6 L_3 L_1 + \lambda_7 L_1^2\left(L_2 - \frac{1+3r_3}{2}L_2^2 - L_3^2\right)$$

$$+\lambda_8 L_2^2\left(L_3-\frac{1+3r_1}{2}L_3^2-L_1^2\right)+\lambda_9 L_3^2\left(L_1-\frac{1+3r_2}{2}L_1^2-L_2^2\right) \tag{6-110}$$

where the 9 basis functions can be called as the modified basis functions.

(2) The normal derivative $\frac{\partial w}{\partial n}$ along each side is a cubic polynomial. If the point conforming conditions are satisfied at the mid-side points and two ends of the side, $\frac{\partial w}{\partial n}$ must satisfy the average line conforming conditions, so this element is a convergent model.

Example 6.12 The deflection and moment of the simply-supported and clamped square plates subjected to uniform load q and central concentrated load P.

Two mesh types are used: mesh A and B in Fig. 6.2. The results by the element MB1-T9 are given in Tables 6.18 and 6.19. It can be seen that this element exhibits good performance.

Table 6.18 The results of the central deflection (MB1-T9)

Mesh (1/4 plate)	Uniform load q				Central concentrated load P			
	Simply-supported		Clamped		Simply-supported		Clamped	
	Mesh A	Mesh B	Mesh A	Mesh B	Mesh A	Mesh B	Mesh A	Mesh B
2×2	0.3969 (−2.3%)	0.4066 (0.1%)	0.1324 (4.7%)	0.1128 (−10.9%)	1.093 (−5.8%)	1.166 (0.5%)	0.5300 (−5.6%)	0.5279 (−5.9%)
4×4	0.4041 (−0.5%)	0.4068 (0.1%)	0.1277 (0.9%)	0.1234 (−2.5%)	1.143 (−1.8%)	1.160 (0.0%)	0.5514 (−1.8%)	0.5526 (−1.5%)
6×6	0.4053 (−0.2%)	0.4066 (0.1%)	0.1270 (0.4%)	0.1251 (−1.1%)	1.152 (−0.8%)	1.160 (0.0%)	0.5564 (−0.9%)	0.5571 (−0.7%)
8×8	0.4057 (−0.1%)	0.4064 (0.0%)	0.1268 (0.2%)	0.1258 (−0.6%)	1.155 (−0.4%)	1.160 (0.0%)	0.5584 (−0.5%)	0.5588 (−0.4%)
Analytical	$0.4062(qL^4/100D)$		$0.1265(qL^4/100D)$		$1.160(PL^2/100D)$		$0.5612(PL^2/100D)$	

6.5.2 Triangular Element MB2-T9

Another triangular element MB2-T9 can be derived by a similar scheme. The difference with the element MB1-T9 is that $\hat{w}$ is re-assumed as follows:

$$\hat{w}=\lambda_{10}L_1^2L_2L_3+\lambda_{11}L_2^2L_3L_1+\lambda_{12}L_3^2L_1L_2 \tag{6-111}$$

From the point conforming conditions of the normal slope ψ_n at the mid-side points, we obtain

$$\begin{Bmatrix}\lambda_{10}\\ \lambda_{11}\\ \lambda_{12}\end{Bmatrix}=\frac{1}{2}\begin{bmatrix}3(1+r_3) & 1-3r_1 & -(1-3r_2)\\ -(1-3r_3) & 3(1+r_1) & 1-3r_2\\ 1-3r_3 & -(1-3r_1) & 3(1+r_2)\end{bmatrix}\begin{Bmatrix}\lambda_7\\ \lambda_8\\ \lambda_9\end{Bmatrix} \tag{6-112}$$

The total deflection w can be expressed in terms of λ_1, λ_2, $\cdots$, λ_9 and their modified basis functions, and its expression is the same as that of the element proposed by Specht[19], but the derivation procedure here is much simpler.

Table 6.19 The results of the central and mid-side moments (MB1-T9)

Mesh (1/4 plate)	Central moment (q)				Mid-side moment (clamped plate)			
	Simply-supported		Clamped		(P)		(q)	
	Mesh A	Mesh B	Mesh A	Mesh B	Mesh A	Mesh B	Mesh A	Mesh B
2×2	0.5468 (14.2%)	0.5477 (14.4%)	0.3077 (34.3%)	0.2720 (18.7%)	−0.1706 (35.7%)	−0.1001 (−20.3%)	−0.0707 (37.8%)	−0.0333 (−35.2%)
4×4	0.5001 (4.4%)	0.4971 (3.8%)	0.2524 (10.2%)	0.2408 (5.1%)	−0.1509 (20.0%)	−0.1162 (−7.6%)	−0.0648 (26.4%)	−0.0429 (−16.4%)
6×6	0.4882 (2.0%)	0.4873 (1.8%)	0.2395 (4.5%)	0.2343 (2.3%)	−0.1439 (14.5%)	−0.1181 (−6.1%)	−0.0613 (19.4%)	−0.0454 (−11.6%)
8×8	0.4828 (0.8%)	0.4837 (1.0%)	0.2350 (2.6%)	0.2319 (1.2%)	−0.1399 (11.3%)	−0.1193 (−5.1%)	−0.0592 (15.4%)	−0.0467 (−9.0%)
Analytical	0.4789(qL^2/10)		0.2291(qL^2/10)		−0.1257(P)		−0.0513(qL^2)	

6.6 SemiLoof Conforming Scheme

This section will introduce the second construction scheme for the super-basis thin plate elements formulated only by the point conforming conditions, i.e. SemiLoof conforming scheme. This scheme is a novel scheme by the combination of the generalized conforming element and the SemiLoof element[20], and possesses the following characteristics:

(1) Unlike the SemiLoof element with DOFs at the corner and mid-side nodes, the elements here only contain DOFs at the corner nodes, which is much simpler and more suitable for applications.

(2) It is not necessary that a one-to-one correspondence exists between the element DOFs and the selected conforming conditions (and a super-basis scheme $m>n$ is used). But, the limit compatibility should be ensured when the mesh is refined by infinite elements, so that the advantages (reliability and convergence) of the generalized conforming elements can be guaranteed.

(3) The integral form conforming conditions (such as line conforming and perimeter conforming conditions), which are usually employed by the generalized conforming elements, are not adopted here. All the conforming conditions used

are discrete point conforming conditions: the point conforming conditions about deflection w at the corner nodes and mid-side points, and the point conforming conditions about the normal slope ψ_n at two Gauss points of each side (the Semi-Loof constraint conditions). So the derivation procedure becomes more convenient.

The no. 19, 20 and 21 elements LSL-T9, LSL-R12 and LSL-Q12 in Table 5.1 belong to this element group, in which two elements LSL-T9[21] and LSL-Q12[22] will be introduced in detail.

6.6.1 Triangular Element LSL-T9

A triangular thin plate element is shown in Fig. 6.16. The nodal displacement vector (element DOFs) $\boldsymbol{q}^e$ is the same as Eq. (6-1).

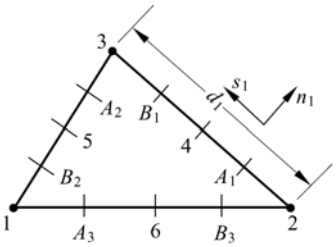

Figure 6.16 A triangular thin plate element with SemiLoof constraint conditions 4,5,6 are mid-side points; and A_i and B_i are two Gauss points along each side

The element deflection field w is assumed to be a polynomial with 12 unknown coefficients, expressible in terms of the area coordinates L_1, L_2 and L_3 as follows

$$\begin{aligned} w = {} & [\lambda_1 L_1 + \lambda_2 L_2 + \lambda_3 L_3] + [\lambda_4 L_2 L_3 + \lambda_5 L_3 L_1 + \lambda_6 L_1 L_2] \\ & + [\lambda_7 L_2 L_3 (L_2 - L_3) + \lambda_8 L_3 L_1 (L_3 - L_1) + \lambda_9 L_1 L_2 (L_1 - L_2)] \\ & + [\lambda_{10} L_1^2 L_2 L_3 + \lambda_{11} L_2^2 L_3 L_1 + \lambda_{12} L_3^2 L_1 L_2] \end{aligned} \tag{6-113}$$

The following 12 point conforming conditions are selected:

$$(w - \tilde{w})_i = 0 \quad (i = 1,2,3) \tag{6-114}$$

$$(w - \tilde{w})_j = 0 \quad (j = 4,5,6) \tag{6-115}$$

$$\left(\frac{\partial w}{\partial n} - \tilde{\psi}_n \right)_k = 0 \quad (k = A_1, B_1, A_2, B_2, A_3, B_3) \tag{6-116}$$

Equations (6-114) and (6-115) are the point conforming conditions about deflection at the corner nodes (nodes 1, 2, 3) and mid-side points (points 4, 5, 6); Eq. (6-116) is the point conforming conditions about the normal slope at Gauss points (points A_1, B_1, A_2, B_2, A_3, B_3) along the element sides.

Firstly, from Eq. (6-114), we obtain

$$\lambda_1 = w_1, \quad \lambda_2 = w_2, \quad \lambda_3 = w_3 \tag{6-117}$$

Secondly, λ_4, λ_5 and λ_6 can be obtained from Eq. (6-115), for example, for the mid-side point 4 of side $\overline{23}$, we have

$$w_4 = \frac{1}{2}\lambda_2 + \frac{1}{2}\lambda_3 + \frac{1}{4}\lambda_4$$
$$\tilde{w}_4 = \frac{1}{2}(w_2 + w_3) + \frac{c_1}{8}(\psi_{x2} - \psi_{x3}) - \frac{b_1}{8}(\psi_{y2} - \psi_{y3})$$

Then, as shown in the first equation below, λ_4 can be solved:

$$\left.\begin{aligned}
\lambda_4 &= \frac{c_1}{2}(\psi_{x2} - \psi_{x3}) - \frac{b_1}{2}(\psi_{y2} - \psi_{y3}) \\
\lambda_5 &= \frac{c_2}{2}(\psi_{x3} - \psi_{x1}) - \frac{b_2}{2}(\psi_{y3} - \psi_{y1}) \\
\lambda_6 &= \frac{c_3}{2}(\psi_{x1} - \psi_{x2}) - \frac{b_3}{2}(\psi_{y1} - \psi_{y2})
\end{aligned}\right\} \tag{6-118}$$

Finally, the rest of the unknown coefficients can be obtained from Eq. (6-116):

$$\left.\begin{aligned}
\lambda_7 &= \frac{1}{2}[(r_2 + r_3)w_1 + (3 - r_3)w_2 - (r_2 + 3)w_3] + \frac{1}{12}[(c_1 - 3r_2c_2 + 3r_3c_3)\psi_{x1} \\
&\quad + (3r_3c_3 - c_3 + 8c_1)\psi_{x2} - (3r_2c_2 + c_2 - 8c_1)\psi_{x3}] - \frac{1}{12}[(b_1 - 3r_2b_2 \\
&\quad + 3r_3b_3)\psi_{y1} + (3r_3b_3 - b_3 + 8b_1)\psi_{y2} - (3r_2b_2 + b_2 - 8b_1)\psi_{y3}] \\
\lambda_8 &= \frac{1}{2}[-(r_3 + 3)w_1 + (r_3 + r_1)w_2 + (3 - r_1)w_3] + \frac{1}{12}[-(3r_3c_3 + c_3 - 8c_2)\psi_{x1} \\
&\quad + (c_2 - 3r_3c_3 + 3r_1c_1)\psi_{x2} + (3r_1c_1 - c_1 + 8c_2)\psi_{x3}] - \frac{1}{12}[-(3r_3b_3 + b_3 \\
&\quad - 8b_2)\psi_{y1} + (b_2 - 3r_3b_3 + 3r_1b_1)\psi_{y2} + (3r_1b_1 - b_1 + 8b_2)\psi_{y3}] \\
\lambda_9 &= \frac{1}{2}[(3 - r_2)w_1 - (r_1 + 3)w_2 + (r_1 + r_2)w_3] + \frac{1}{12}[(3r_2c_2 - c_2 + 8c_3)\psi_{x1} \\
&\quad - (3r_1c_1 + c_1 - 8c_3)\psi_{x2} + (c_3 - 3r_1c_1 + 3r_2c_2)\psi_{x3}] - \frac{1}{12}[(3r_2b_2 - b_2 \\
&\quad + 8b_3)\psi_{y1} - (3r_1b_1 + b_1 - 8b_3)\psi_{y2} + (b_3 - 3r_1b_1 + 3r_2b_2)\psi_{y3}] \\
\lambda_{10} &= \lambda_{11} = \lambda_{12} = (r_3 - r_2)w_1 + (r_1 - r_3)w_2 + (r_2 - r_1)w_3 \\
&\quad + \frac{1}{2}[(r_2c_2 + r_3c_3)\psi_{x1} + (r_3c_3 + r_1c_1)\psi_{x2} + (r_1c_1 + r_2c_2)\psi_{x3}] \\
&\quad - \frac{1}{2}[(r_2b_2 + r_3b_3)\psi_{y1} + (r_3b_3 + r_1b_1)\psi_{y2} + (r_1b_1 + r_2b_2)\psi_{y3}]
\end{aligned}\right\} \tag{6-119}$$

where b_i, c_i and r_i are given in Eq. (6-58).

Once $\boldsymbol{\lambda}$ is solved and expressed in terms of $\boldsymbol{q}^e$, the element stiffness matrix can be derived following the conventional procedure. Note that the element LT in reference [23] derived with the integral conforming conditions is equivalent to the present element. However, the construction procedure in this section based on the point conforming conditions appears to be simpler, and is easy to be extended to formulate quadrilateral element.

Example 6.13 The central deflection and central moment of the simply-supported and the clamped square plates subjected to uniform load.

Results by the elements LSL-T9 and CT proposed by Fricker[11] are given in Table 6.20 for comparison. It can be seen that the accuracy of the present element is better than that of the element CT (Meshes *A* and *B* in Fig. 6.2 are used).

Table 6.20 The central deflection and moment of square plates subjected to uniform load (LSL-T9)

	Mesh (1/4 plate)	Simply-supported				Clamped			
		LST-T9		CT		LST-T9		CT	
		Mesh *A*	Mesh *B*	Mesh *A*	Mesh *B*	Mesh *A*	Mesh *B*	Mesh *A*	Mesh *B*
Central deflection	2×2	0.4014 (−1.2%)	0.4024 (−0.9%)	0.399 30 (−1.7%)	0.351 18 (−13.6%)	0.122 88 (−2.9%)	0.107 68 (−14.9%)	0.147 50 (16.6%)	0.107 32 (−15.2%)
	4×4	0.4051 (−0.3%)	0.4058 (−0.1%)	0.404 39 (−0.5%)	0.392 80 (−3.3%)	0.125 44 (−0.8%)	0.122 03 (−3.6%)	0.132 21 (4.5%)	0.122 32 (−3.3%)
	6×6	0.405 74 (−0.1%)	0.406 09 (−0.03%)	0.405 40 (−0.2%)	0.400 28 (−1.5%)	0.126 11 (−0.3%)	0.124 52 (−1.6%)	0.129 12 (2.0%)	0.124 68 (−1.5%)
	Analytical	0.406 235$qL^4/(100D)$				0.126 53$qL^4/(100D)$			
Central moment	2×2	0.5022 (4.9%)	0.5161 (7.8%)	0.499 88 (4.4%)	0.439 58 (−8.2%)	0.2909 (27%)	0.2380 (3.9%)	0.295 10 (28.8%)	0.205 27 (−10.4%)
	4×4	0.4798 (0.2%)	0.4917 (2.7%)	0.483 47 (1.0%)	0.470 05 (−1.8%)	0.2386 (4.2%)	0.2343 (2.3%)	0.246 71 (7.7%)	0.223 89 (−2.3%)
	6×6	0.478 21 (−0.1%)	0.485 51 (1.4%)	0.480 90 (0.4%)	0.474 93 (−0.8%)	0.232 77 (1.6%)	0.231 55 (1.1%)	0.237 51 (3.7%)	0.226 05 (−1.3%)
	Analytical	0.478 86($qL^2/10$)				0.229 05($qL^2/10$)			

6.6.2 Quadrilateral Element LSL-Q12

A quadrilateral thin plate element with 12 conventional DOFs is shown in Fig. 6.17. Its nodal displacement vector $\boldsymbol{q}^e$ is

$$\boldsymbol{q}^e = [w_1 \quad \psi_{x1} \quad \psi_{y1} \quad w_2 \quad \psi_{x2} \quad \psi_{y2} \quad w_3 \quad \psi_{x3} \quad \psi_{y3} \quad w_4 \quad \psi_{x4} \quad \psi_{y4}]^{\mathrm{T}} \tag{6-120}$$

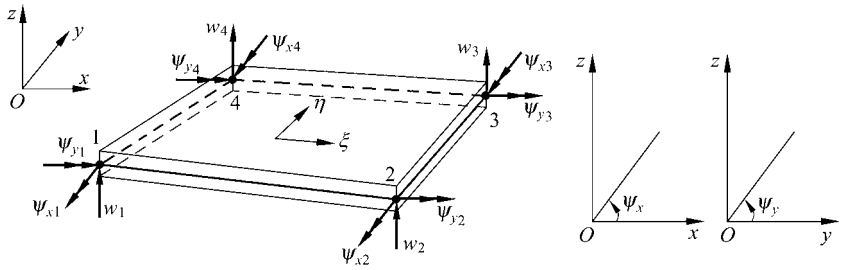

Figure 6.17 A quadrilateral thin plate element

The element deflection w is assumed to be a polynomial with 16 unknown coefficients, and expressed in terms of ξ and η as

$$\begin{aligned} w = {} & \lambda_1 + \lambda_2\xi + \lambda_3\eta + \lambda_4\xi\eta + (\xi^2-1)(\lambda_5 + \lambda_6\eta) + (\eta^2-1)(\lambda_7 + \lambda_8\xi) \\ & + \xi(\xi^2-1)(\alpha_1 + \alpha_3\eta) + \eta(\eta^2-1)(\alpha_2 + \alpha_4\xi) + (\xi^2-1)(\eta^2-1)(\alpha_5 + \alpha_6\xi + \alpha_7\eta) \\ & + \alpha_8[\xi^2(\xi^2-1) - \eta^2(\eta^2-1)] \end{aligned} \tag{6-121}$$

Apply the following 16 conforming conditions

$$(w - \tilde{w})_i = 0 \quad (i = 1,2,\cdots,8) \tag{6-122}$$

$$\left(\frac{\partial w}{\partial n} - \tilde{\psi}_n\right)_j = 0 \quad (j = A_1, B_1, A_2, B_2, A_3, B_3, A_4, B_4) \tag{6-123}$$

where Eq. (6-122) denotes the point conforming conditions about deflections at the corner nodes (nodes 1, 2, 3 and 4) and the mid-side points (points 5, 6, 7 and 8); Eq. (6-123) denotes the point conforming conditions about the normal slopes at eight Gauss points $A_j\left(\xi_j, \frac{1}{\sqrt{3}}\eta_j\right)$ and $B_j\left(\frac{1}{\sqrt{3}}\xi_j, \eta_j\right)$ (j = 1, 2, 3, 4) along the four element sides. These 16 point conforming conditions are the SemiLoof constraint conditions[20], as shown in Fig. 6.18.

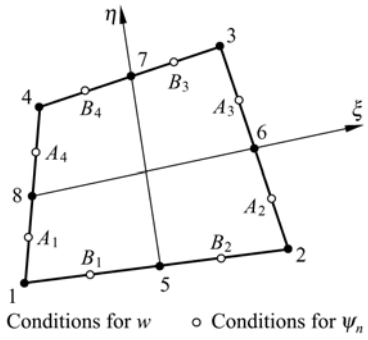

Figure 6.18 SemiLoof constraint conditions

Firstly, by applying the condition (6-122), $\lambda_1, \lambda_2, \cdots, \lambda_8$ can be solved as follows:

$$\left.\begin{aligned}
&\lambda_1 = \frac{1}{4}\sum_{i=1}^{4} w_i, \qquad \lambda_2 = \frac{1}{4}\sum_{i=1}^{4} w_i\xi_i \\
&\lambda_3 = \frac{1}{4}\sum_{i=1}^{4} w_i\eta_i, \qquad \lambda_4 = \frac{1}{4}\sum_{i=1}^{4} w_i\xi_i\eta_i \\
&\lambda_5 = \frac{1}{8}\sum_{i=1}^{4}[\psi_{xi}\xi_i(\bar{a}_1 + \bar{a}_3\eta_i) + \psi_{yi}\xi_i(\bar{b}_1 + \bar{b}_3\eta_i)] \\
&\lambda_6 = \frac{1}{8}\sum_{i=1}^{4}[\psi_{xi}\xi_i(\bar{a}_1\eta_i + \bar{a}_3) + \psi_{yi}\xi_i(\bar{b}_1\eta_i + \bar{b}_3)] \\
&\lambda_7 = \frac{1}{8}\sum_{i=1}^{4}[\psi_{xi}\eta_i(\bar{a}_2 + \bar{a}_3\xi_i) + \psi_{yi}\eta_i(\bar{b}_2 + \bar{b}_3\xi_i)] \\
&\lambda_8 = \frac{1}{8}\sum_{i=1}^{4}[\psi_{xi}\eta_i(\bar{a}_2\xi_i + \bar{a}_3) + \psi_{yi}\eta_i(\bar{b}_2\xi_i + \bar{b}_3)]
\end{aligned}\right\} \tag{6-124}$$

where

$$\left.\begin{aligned}
&\bar{a}_1 = \frac{1}{4}\sum_{i=1}^{4} x_i\xi_i, \quad \bar{a}_2 = \frac{1}{4}\sum_{i=1}^{4} x_i\eta_i, \quad \bar{a}_3 = \frac{1}{4}\sum_{i=1}^{4} x_i\xi_i\eta_i \\
&\bar{b}_1 = \frac{1}{4}\sum_{i=1}^{4} y_i\xi_i, \quad \bar{b}_2 = \frac{1}{4}\sum_{i=1}^{4} y_i\eta_i, \quad \bar{b}_3 = \frac{1}{4}\sum_{i=1}^{4} y_i\xi_i\eta_i
\end{aligned}\right\} \tag{6-125}$$

Secondly, $\alpha_1, \alpha_2, \cdots, \alpha_8$ can be solved from the condition (6-123). And, their expressions are given in reference [22].

Now, all the unknown coefficients are solved, the element stiffness matrix can be derived following the conventional procedure.

Example 6.14 The central deflection of a simply-supported circular plate subjected to uniform load. For comparison, results by the triangular element proposed by Felippa and Bergan[14] are also given together with those of the present element LSL-Q12. The Poisson's ratio $\mu = 0.3$.

Owing to symmetry, only one quarter plate is calculated. The two meshes in Fig. 6.14 are used again, in which mesh *A* contains 12 quadrilateral or 24 triangular elements, and mesh *B* contains 48 quadrilateral or 96 triangular elements.

The computational errors are given in Table 6.21. It can be seen that the precision of the element LSL-Q12 is better than that of the triangular element in reference [14].

Table 6.21 The computational errors for central deflection of a simply-supported circular plate (uniform load)

Mesh for 1/4 circular plate	LSL-Q12	Triangular element[14]
Mesh *A*	0.66%	2.87%
Mesh *B*	0.17%	0.70%

Example 6.15 The central deflection and moment of the simply-supported and the clamped square plates (the length of side is L) subjected to uniform load. The Poisson's ratio is 0.3.

Three Meshes A, B and C in Fig. 6.19 are used for one quarter plate. And, the results are given in Table 6.22. It can be seen that the element LSL-Q12 possesses high precision for both regular and irregular meshes.

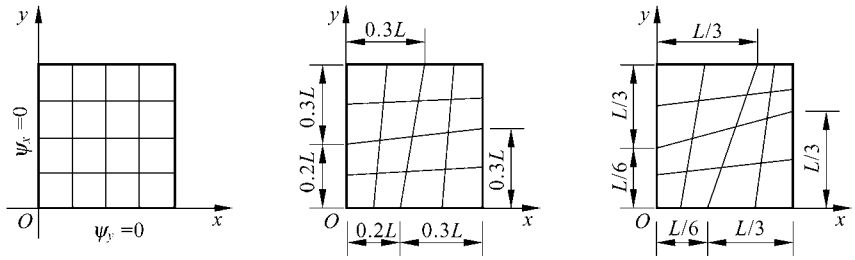

Figure 6.19 Meshes for 1/4 plate

(a) Mesh A 4 × 4; (b) Mesh B 4 × 4; (c) Mesh C 4 × 4

Table 6.22 Results by element LSL-Q12 for square plates subjected to uniform load

	Mesh (1/4 plate)	Simply-supported			Clamped		
		Mesh A	Mesh B	Mesh C	Mesh A	Mesh B	Mesh C
Central deflection	2 × 2	0.405 13 (−0.27%)	0.404 42 (−0.45%)	0.403 10 (−0.77%)	0.122 65 (−3.07%)	0.122 34 (−3.31%)	0.121 18 (−4.23%)
	4 × 4	0.406 16 (−0.02%)	0.406 11 (−0.03%)	0.405 96 (−0.07%)	0.125 86 (−0.53%)	0.125 75 (−0.62%)	0.125 72 (−0.64%)
	8 × 8	0.406 23 (0.00%)	0.406 14 (−0.02%)	0.405 74 (−0.12%)	0.126 44 (−0.07%)	0.126 41 (−0.09%)	0.126 39 (−0.11%)
	Analytical	$0.406\,235qL^4/(100D)$			$0.126\,53qL^4/(100D)$		
Central moment	2 × 2	0.512 43 (7.01%)	0.518 02 (8.18%)	0.526 91 (10.03%)	0.257 28 (12.32%)	0.254 25 (11.00%)	0.258 85 (13.01%)
	4 × 4	0.487 30 (1.76%)	0.486 69 (1.64%)	0.486 56 (1.61%)	0.236 80 (3.38%)	0.235 27 (2.72%)	0.234 63 (2.44%)
	8 × 8	0.480 98 (0.44%)	0.480 38 (0.32%)	0.479 60 (0.15%)	0.231 07 (0.88%)	0.230 47 (0.62%)	0.230 14 (0.48%)
	Analytical	$0.478\,86qL^2/10$			$0.229\,05qL^2/10$		

Example 6.16 The central deflection w and central moment M_y of a rhombus plate (Fig. 6.15) subjected to uniform load.

The results of central deflection and moment by the element LSL-Q12 and other models are listed in Table 6.23. Compared with the elements in references [15, 16], LSL-Q12 has better precision.

Table 6.23 The central deflection and central moment of a rhombus plate subjected to uniform load

DOF	Mesh	Central deflection w			Central moment M_y		
		LSL-Q12	[15]	[16]	LSL-Q12	[15]	[16]
27	2 × 2	0.7637	0.7230		1.0006	0.7602	
75	4 × 4	0.7872	0.7718	0.8414	1.0372	0.9172	0.9761
105	4 × 6	0.7904	0.7850		0.9478	0.9473	
243	8 × 8	0.7918		0.8111	0.9777		0.9739
507	12 × 12	0.7927		0.8057	0.9680		0.9688
Difference method[15]		$0.7945qL^4/(100D)$			$0.9589qL^2/10$		

References

[1] Bazeley GP, Cheung YK, Irons BM, Zienkiewicz OC (1965) Triangular elements in bending-conforming and nonconforming solution. In: Proceedings of the Conference on Matrix Methods in Structural Mechanics. Air Force Institute of Technology, Ohio: Wright-Patterson A. F. Base pp 547 – 576

[2] Batoz JL, Bathe KJ, Ho LW (1980) A study of three-node triangular plate bending elements. International Journal for Numerical Methods in Engineering 15: 1771 – 1812

[3] Stricklin JA, Haisler WE, Tisdale PR, Gunderson R (1969) A rapidly converging triangular plate element. AIAA Journal 7: 180 – 181

[4] Allman DJ (1971) Triangular finite element plate bending with constant and linearly varying bending moments. In: BF de Veubeke (ed) High Speed Computing of Elastic Structures. Liege Belgium, pp105 – 136

[5] Clough RW, Tocher JL (1965) Finite element stiffness matrices for analysis of plate bending. In: Proceedings of the Conference on Matrix Methods in Structural Mechanics. Air Force Institute of Technology, Ohio: Wright-Patterson A. F. Base, pp515 – 545

[6] Melosh RJ (1963) Basis for derivation of matrices for the direct stiffness method. AIAA Journal 1(7): 1631 – 1637

[7] Tocher JL, Kapur KK (1965) Comment on "basis of derivation of matrices for direct stiffness method". AIAA Journal 3(6): 1215 – 1216

[8] Kapur KK, Hartz BJ (1966) Stability of thin plates using the finite element method. In: Proceedings of American Socity of Civil Engineering, pp177 – 195

[9] Xu Y, Long ZF (1995) A simple generalized conforming rectangular plate bending element. In: Proceedings of the Fourth National Conference on Structural Engineering, pp315 – 319 (in Chinese)

[10] Long ZF (1993) Generalized conforming triangular elements for plate bending. Communications in Numerical Methods in Engineering 9: 53 – 65

[11] Fricker AJ (1985) An improved three-node triangular element for plate bending. International Journal for Numerical Methods in Engineering 21: 105 – 114

[12] Jeyachandrabose C, Kirkhope J (1986) Construction of new efficient three-node triangular thin plate bending elements. Computers & Structures 23(5): 587 – 603
[13] Long YQ, Bu XM, Long ZF, Xu Y (1995) Generalized conforming plate bending elements using point and line compatibility conditions. Computers & Structures 54(4): 717 – 723
[14] Felippa CA, Bergan PG (1987) Triangular bending FE based on energy-orthogonal free formulation. Computer Methods in Applied Mechanics and Engineering 61: 129 – 160
[15] Razzaque A (1973) Program for triangular bending element with derivative smoothing. International Journal for Numerical Methods in Engineering 6: 333 – 343
[16] Zienkiewicz OC, Lefebvre D (1988) A robust triangular plate bending element of the Reissner-Mindlin type. International Journal for Numerical Methods in Engineering 26: 1169 – 1184
[17] Long YQ, Bu XM (1990) A family of efficient elements for thin plate bending. Journal of Tsinghua University 30(5): 9 – 15 (in Chinese)
[18] Long ZF (1991) Low-order and high-precision triangular elements for plate bending. In: Cheung, Lee & Leung (eds) Computational Mechanics. Rotterdam: Balkema, pp1793 – 1797
[19] Specht B (1988) Modified shape functions for the three-node plate bending element passing the patch test. International Journal for Numerical Methods in Engineering 26: 705 – 715
[20] Irons BM (1976) The SemiLoof shell element. In: Gallagher RH, Ashwell DG (eds) Finite Element for Thin and Curved Member. Wiley, pp197 – 222
[21] Long ZF (1992) Two generalized conforming plate elements based on SemiLoof constraints. Computers & Structures 9(1): 53 – 65
[22] Long ZF (1993) Generalized conforming quadrilateral plate element by using SemiLoof constraints. Communications in Numerical Methods in Engineering 9: 417 – 426
[23] Long ZF (1992) Triangular and rectangular plate elements based on generalized compatibility conditions. Computational Mechanics 10(3/4): 281 – 288